THESIS ABSTRACT

EFFECTS OF pH, SURFACE AREA, AND BACKGROUND MATRICES ON THE REMOVAL OF LEAD FROM AQUEOUS SOLUTIONS USING ACTIVATED ALUMINA

Patrick Wootton

Master of Science, June 11, 1999

(Bachelor of Civil Engineering, Auburn University, 1997)

124 Typed pages

Directed by Clifford Lange and Timothy Kramer

The metallic compound lead poses a human health risk and is environmentally toxic. The removal of lead from drinking and waste waters is therefore of great importance. To ensure that the lead concentration is reduced to safe levels, conventional treatment procedures for the removal of lead such as chemical precipitation and ion exchange have been used. These methods often do not yield sufficient removal of lead and can be expensive due to the high costs of required chemicals . Aluminum oxide, Al_2O_3, has been shown to sorb lead from aqueous solutions by concentrating lead at the particle surfaces. Sorption of lead using aluminum oxide (alumina) is effected by many factors,

REPORT DOCUMENTATION PAGE

Form Approved
OMB No. 0704-0188

1. AGENCY USE ONLY *(Leave blank)*	2. REPORT DATE	3. REPORT TYPE AND DATES COVERED
	5.Dec.99	THESIS

4. TITLE AND SUBTITLE
THE EFFECTS OF PH, SURFACE AREA, AND BACKGROUND MATRICES ON THE REMOVAL OF LEAD FROM AQUEOUS SOLUTIONS USING ACTIVATED ALUMINA

5. FUNDING NUMBERS

6. AUTHOR(S)
2D LT WOOTTON PATRICK D

7. PERFORMING ORGANIZATION NAME(S) AND ADDRESS(ES)
AUBURN UNIVERSITY MAIN CAMPUS

8. PERFORMING ORGANIZATION REPORT NUMBER

9. SPONSORING/MONITORING AGENCY NAME(S) AND ADDRESS(ES)
THE DEPARTMENT OF THE AIR FORCE
AFIT/CIA, BLDG 125
2950 P STREET
WPAFB OH 45433

10. SPONSORING/MONITORING AGENCY REPORT NUMBER
FY99-440

11. SUPPLEMENTARY NOTES

12a. DISTRIBUTION AVAILABILITY STATEMENT
Unlimited distribution
In Accordance With AFI 35-205/AFIT Sup 1

12b. DISTRIBUTION CODE

13. ABSTRACT *(Maximum 200 words)*

14. SUBJECT TERMS

15. NUMBER OF PAGES
124

16. PRICE CODE

17. SECURITY CLASSIFICATION OF REPORT	18. SECURITY CLASSIFICATION OF THIS PAGE	19. SECURITY CLASSIFICATION OF ABSTRACT	20. LIMITATION OF ABSTRACT

THESIS ABSTRACT

EFFECTS OF pH, SURFACE AREA, AND BACKGROUND MATRICES ON THE REMOVAL OF LEAD FROM AQUEOUS SOLUTIONS USING ACTIVATED ALUMINA

Patrick Wootton

Master of Science, June 11, 1999

(Bachelor of Civil Engineering, Auburn University, 1997)

124 Typed pages

Directed by Clifford Lange and Timothy Kramer

The metallic compound lead poses a human health risk and is environmentally toxic. The removal of lead from drinking and waste waters is therefore of great importance. To ensure that the lead concentration is reduced to safe levels, conventional treatment procedures for the removal of lead such as chemical precipitation and ion exchange have been used. These methods often do not yield sufficient removal of lead and can be expensive due to the high costs of required chemicals . Aluminum oxide, Al_2O_3, has been shown to sorb lead from aqueous solutions by concentrating lead at the particle surfaces. Sorption of lead using aluminum oxide (alumina) is effected by many factors,

including pH, available surface area, and background compounds or matrices. Each of these variables significantly impacts both the rate of sorption and the equilibrium amount of lead sorbed on the alumina surface.

In this investigation, factors effecting the sorption of lead using alumina were quantified. These factors included the influence of solution pH, alumina surface area (particle size), and presence of background matrices. The specific variables examined were pH solutions that ranged from very acidic (<3.0) to caustic (>8.0), alumina particle sizes of >16 (1190 microns) and <200 (74 microns) mesh sizes, and background matrices containing 1.0 mM acetic acid and 0.1 mM sodium chloride. Equilibrium isotherm studies were conducted over the range of variables using known concentrations of alumina and lead in aqueous solutions.

The isotherm data was plotted as the percentage of lead removed versus mass of alumina. The kinetic data was expressed as the percentage of lead removed versus time. The results specifically showed that the amount and rate of lead sorption was greater at higher pH than for lower pH values. Further, the equilibrium quantity and rate of lead sorption was greater for the fine mesh alumina than for the coarse mesh alumina particles. Background matrices were also found to be detrimental to both equilibrium and rate of lead sorption on activated alumina. The results of this investigation conclude that solution pH plays the most significant role in lead sorption, but alumina particle size and background matrices also decrease the quantity and rate of lead sorption using activated alumina.

including pH, available surface area, and background compounds or matrices. Each of these variables significantly impacts both the rate of sorption and the equilibrium amount of lead sorbed on the alumina surface.

In this investigation, factors effecting the sorption of lead using alumina were quantified. These factors included the influence of solution pH, alumina surface area (particle size), and presence of background matrices. The specific variables examined were pH solutions that ranged from very acidic (<3.0) to caustic (>8.0), alumina particle sizes of >16 (1190 microns) and <200 (74 microns) mesh sizes, and background matrices containing 1.0 mM acetic acid and 0.1 mM sodium chloride. Equilibrium isotherm studies were conducted over the range of variables using known concentrations of alumina and lead in aqueous solutions.

The isotherm data was plotted as the percentage of lead removed versus mass of alumina. The kinetic data was expressed as the percentage of lead removed versus time. The results specifically showed that the amount and rate of lead sorption was greater at higher pH than for lower pH values. Further, the equilibrium quantity and rate of lead sorption was greater for the fine mesh alumina than for the coarse mesh alumina particles. Background matrices were also found to be detrimental to both equilibrium and rate of lead sorption on activated alumina. The results of this investigation conclude that solution pH plays the most significant role in lead sorption, but alumina particle size and background matrices also decrease the quantity and rate of lead sorption using activated alumina.

EFFECTS OF pH, SURFACE AREA, AND BACKGROUND MATRICES ON THE REMOVAL OF LEAD FROM AQUEOUS SOLUTIONS USING ACTIVATED ALUMINA

Patrick Wootton

Certificate of Approval:

Clifford Lange, Co-Chairman
Associate Professor
Civil Engineering

Timothy Kramer, Co-Chairman
Assistant Professor
Civil Engineering

Joe Morgan
Associate Professor
Civil Engineering

Larry Benefield
Professor
Civil Engineering

John F. Pritchett
Dean
Graduate School

EFFECTS OF pH, SURFACE AREA, AND BACKGROUND MATRICES ON THE REMOVAL OF LEAD FROM AQUEOUS SOLUTIONS USING ACTIVATED ALUMINA

Patrick Wootton

A Thesis

Submitted to

the Graduate Faculty of

Auburn University

In Partial Fulfillment of the

Requirements for the

Degree of

Master of Science

Auburn, Alabama

June 11, 1999

EFFECTS OF pH, SURFACE AREA, AND BACKGROUND MATRICES ON THE REMOVAL OF LEAD FROM AQUEOUS SOLUTIONS USING ACTIVATED ALUMINA

Patrick Wootton

Patrick Wootton
Signature of Author

June 11, 1999
Date

Copy sent to:

Name Date

VITA

Patrick David Wootton, son of David R. and Pamela M. Wootton, was born January 1, 1974, in Birmingham, Alabama. He graduated from Thompson High School in Alabaster, Alabama in 1992. He entered Auburn University in September, 1992. At Auburn, he graduated *summa cum laude* with a Bachelor of Civil Engineering in June, 1997. He entered graduate school at Auburn University in September, 1997.

THESIS ABSTRACT

EFFECTS OF pH, SURFACE AREA, AND BACKGROUND MATRICES ON THE REMOVAL OF LEAD FROM AQUEOUS SOLUTIONS USING ACTIVATED ALUMINA

Patrick Wootton

Master of Science, June 11, 1999

(Bachelor of Civil Engineering, Auburn University, 1997)

124 Typed pages

Directed by Clifford Lange and Timothy Kramer

The metallic compound lead poses a human health risk and is environmentally toxic. The removal of lead from drinking and waste waters is therefore of great importance. To ensure that the lead concentration is reduced to safe levels, conventional treatment procedures for the removal of lead such as chemical precipitation and ion exchange have been used. These methods often do not yield sufficient removal of lead and can be expensive due to the high costs of required chemicals . Aluminum oxide, Al_2O_3, has been shown to sorb lead from aqueous solutions by concentrating lead at the particle surfaces. Sorption of lead using aluminum oxide (alumina) is effected by many factors,

including pH, available surface area, and background compounds or matrices. Each of these variables significantly impacts both the rate of sorption and the equilibrium amount of lead sorbed on the alumina surface.

In this investigation, factors effecting the sorption of lead using alumina were quantified. These factors included the influence of solution pH, alumina surface area (particle size), and presence of background matrices. The specific variables examined were pH solutions that ranged from very acidic (<3.0) to caustic (>8.0), alumina particle sizes of >16 (1190 microns) and <200 (74 microns) mesh sizes, and background matrices containing 1.0 mM acetic acid and 0.1 mM sodium chloride. Equilibrium isotherm studies were conducted over the range of variables using known concentrations of alumina and lead in aqueous solutions.

The isotherm data was plotted as the percentage of lead removed versus mass of alumina. The kinetic data was expressed as the percentage of lead removed versus time. The results specifically showed that the amount and rate of lead sorption was greater at higher pH than for lower pH values. Further, the equilibrium quantity and rate of lead sorption was greater for the fine mesh alumina than for the coarse mesh alumina particles. Background matrices were also found to be detrimental to both equilibrium and rate of lead sorption on activated alumina. The results of this investigation conclude that solution pH plays the most significant role in lead sorption, but alumina particle size and background matrices also decrease the quantity and rate of lead sorption using activated alumina.

ACKNOWLEDGEMENTS

I wish to extend my sincere thanks and appreciation to the following individuals. My chairmen, Dr. Clifford Lange and Dr. Timothy Kramer for providing both leadership and support throughout my time at Auburn. Their knowledge of laboratory and experimental methods has been invaluable to my progress. Their writing skills and ability to organize ideas and information allowed me to present my work in a concise manner. Dr. Larry Benefield, Dr. Joe Morgan, and Dr. Joe Judkins who always had the time to answer all of my questions ranging from academic concerns to Auburn athletics.

The AFIT program for providing me this opportunity to work on my degree at Auburn University. The entire staff at Detachment 005 who have looked out for my best interests while at Auburn. The Air Force Association for helping to fund my education.

My fellow graduate students for exhibiting the spirit of teamwork rather than competition in the classroom and laboratory.

My parents and sister, Dave, Pam, and Kimberly Wootton, for their understanding and support throughout my life. The lessons that they taught me have made me the person I am today. Finally, to Allison Wootton, the greatest wife in the world. Her understanding and care made my successes possible. No one has sacrificed more so that I could be successful over the past two years.

Style or manual or journal used ___ ASCE Author's Guide to Journals, Books, and Reference Publications

Computer software used Microsoft Office 97 – Microsoft Word, Microsoft Excel, and Jandel Sigma Plot

TABLE OF CONTENTS

LIST OF TABLES

LIST OF FIGURES

1.INTRODUCTION

Heavy metals found in surface and ground waters are toxic to aquatic biota and present a threat to human health (Reed and Arunachalam, 1994). Heavy metals are detrimental to the chemistry of water which in turn adversely effects the wildlife and vegetation in the streams (Ahmed, *et al.*, 1998). One metal of extreme interest is lead. Lead is classified as a primary pollutant by the United States Environmental Protection Agency (USEPA) (Reed and Arunachalam, 1994). Although, lead is not as toxic as some heavy metals, it is a cumulative toxin that remains in the body, concentrating over time. Long-term exposure to lead can lead to gastrointestinal track and nervous system disorders (Orunwense, 1996).

Toxic heavy metal pollutants are generated through military, industrial, mining, and agricultural activities. According to Brower (1997), energy production industries generate 2.4 million tons of heavy metals per year. The metals identified by Brower include As, Cd, Cr, Cu, Hg, Ni, Pb, Se, V, and Zn. Metal processing industries are responsible for 0.39 million tons annually; agricultural generates 1.4 million tons annually; manufacturing industry generates 0.24 million tons annually; and the waste disposal industry is responsible for 0.72 million tons annually. Individual sources of concern for heavy metal contamination include electroplating,

metal finishing industries, metallurgical industries, tannery operations, chemical manufacturing, mine draining, electric battery manufacturing, leachates from landfills, and contaminated groundwater from hazardous waste sites (Reed and Arunachalam, 1994). Lead has been identified as a contaminate in more than 1/3 of the 1200 superfund sites on the National Priority List (Wei and Huang, 1998). Lead was also added to motor fuels to increase octane ratings and subsequently discharged to the atmosphere during combustion (Orumwense, 1996). Once lead is in the atmosphere it is delivered to natural waters through precipitation. Studies have shown that lead levels are directly related to the degree of industrialization in a particular area. Lead is also capable of binding to soil particles and eventually distributed throughout natural receiving waters via sediment runoff and soil erosion. The mechanism of soil binding is also responsible for the fate of lead contamination throughout groundwater once the lead reaches these underground aquifers.

There are numerous methods of removing heavy metals from aqueous solutions. Ion exchange, reverse osmosis, chemical oxidation, solvent extraction, membrane separation, and electrowinning are methods that have been used. Although these technologies are effective to a certain degree, each have problems such as excessive costs or large volumes of sludge formed from the process (Brower, 1997). A popular method for removing most heavy metals is chemical precipitation. One major drawback to using precipitation for toxic metal removal is that most aqueous wastes contain competing substances, such as complexing agents, that decrease the effectiveness of precipitation (Reed and Arunachalam, 1994). The introduction of

solid, sorbent particles, such as aluminum oxides or activated carbon, provide inexpensive methods of removing metals from solution. Sorption of heavy metals onto these solid particles can be used as primary, secondary or tertiary processes in treatment plants. Further, sorption processes can be used effectively when the metal concentration is extremely low (Reed and Arunachalam, 1994).

One such sorption process occurs with aluminum oxide (Al_2O_3). Aluminum oxide (alumina) is inexpensive and found in large quantities from natural deposits. Alcoa has found that sorption processes using alumina compete favorably against ion exchange, electrolysis, and can sorb virtually any metal to some degree (Goodboy and Fleming, 1984). In addition, the alumina can be efficiently regenerated, further lowering treatment costs. Alumina typically comes in a granular form, but may be produced as a fine powdered form. Powdered alumina can thus be used in a continuously stirred tank reactor to remove metals from solution by sorption, and subsequently sedimentation and/or filtration.

The goal of using alumina as an effective metals removal process envisioned by this research is to add powdered alumina in a batch tank reactor to remove metals from solution. The alumina particles with the metal ions sorbed to its surface could then be captured by a ultra-membrane filtration system. The use of powdered alumina for water treatment has already taken place in some locations. The California Department of Corrections used a combination of activated alumina and reverse osmosis to remove metals from potable water (Lee and Hargreaves, 1995). The purpose of this investigation is to focus on the removal of lead using activated

alumina. Emphasis will be placed on the effects of several variables: pH, alumina particle size, and the presence of background matrices on lead removal using activated alumina. The dependent variables for the investigation will be the capacity of lead sorbed onto the alumina and rate at which the lead is removed from solution.

2. LITERATURE REVIEW

2.1 ALUMINUM OXIDE

2.1.1 Background

Aluminum is the most common metal in the environment and aluminum oxide (alumina) is the most common form of aluminum. Over the past 70 years, aluminum has been used as a sorbent in a number of environmental processes. In this section, the history, types, safety, and availability of alumina are reviewed.

2.1.2 History and Uses of Alumina

Aluminum oxide (Al_2O_3), also known as alumina, has been used for various purposes during the past century. Goodboy and Fleming (1984) provided a rigorous summary of the development and application of alumina from a desiccant to an effective sorbent. Earliest known uses of alumina was for chromatographic separation of liver extracts by Folkers and Shovel in 1901. Alcoa introduced alumina commercially for water adsorption in 1932. Successful application of alumina was first achieved as a desiccant for water adsorption in chemical processes for gases and liquids. Until 1940, sorbent aluminas were primarily used for both air and natural gas dehydration processes. In the 1950's and 1960's, alumina began to be used for more advanced purposes. These two decades saw alumina applied to isotopic separation of actinide series compounds and

removal of impurities in halogenated compounds. The 1970's saw drastic changes in the use of alumina. Instead of using alumina for drying purposes, alumina began to be applied as an effective sorbent in removing contaminants from potable water processes. In the 1970's, alumina was used to remove such constituents as phosphate, mercaptan, and fluoride and less than half of the alumina by volume was being used for desiccant purposes. Alumina extensively moved into the petroleum industry in the 1980's for the adsorption of acidic gases and sulfur species. Alumina continues to be used in new and innovative ways. Recently alumina has been incorporated in municipal wastewater treatment, drinking water treatment, polymer science, and pharmaceutical technologies.

2.1.3 Classifications of Alumina Species

Aluminum oxides can be classified into several unique categories. First, they can be classified by their double layer arrangements. The double layer classification is denoted by a Greek lettering system introduced by Alcoa in 1930 (Papee and Tertian, 1963). Aluminas can be further subdivided by the number of water molecules attached to the aluminum oxide particle. The number of water molecules is noted by trihydrate or monohydrate aluminas. Particle structure can define the type of alumina. Particles of alumina can be either an amorphous or crystalline structure, or a transition alumina that falls somewhere between the two forms.

Amorphous alumina structures lack definite shape or crystalline form. By definition, amorphous aluminas have greater concentrations of crystal defect structures than the more structured transition aluminas (Goodboy and Fleming, 1984). The transition aluminas lie between the amorphous structures and the pure crystalline structures in

molecular order. Crystalline aluminas are formed at high temperatures and have well ordered, definitive molecular structure.

Transition alumina forms are dependent on the arrangement of Al^{3+} and O^{2-} ions in the crystal lattice. The lattice arrangement can be tetrahedrally or octahedrally in cubic or hexagonal, tightly packed systems (Goodboy and Fleming, 1984). This transition phase arrangement occurs before the amorphous structure takes on a crystalline shape. During this transition, a rearrangement of anion and cation sublattice takes place forming many defect structures. The largest group of adsorbents are the transition forms. In fact, the majority of alumina products available to the public lie in the transition category due to the beneficial properties of the defect structures formed during this transition phase (Goodboy and Fleming, 1984).

Aluminum is the most common metal in the environment and alumina is the most common form of aluminum. The Bayer process is a method used to form alumina compounds by precipitation from an aluminate solution (Goodboy and Fleming, 1984). The term "activated" alumina describes adsorption aluminas formed by heating the product of the Bayer process (Edwards and Bayha, 1947). Activated aluminas have pores produced by heating the aluminum hydrates to temperatures sufficient to drive off water molecules that are attached to the particles. The earliest commercial form of adsorptive alumina is Bayer α-trihydrate which is formed by heating particles to 400°C to activate the particles (Papee and Tertian, 1963). The activated aluminas possess both Lewis and Bronsted acidic and basic sites (Goodboy and Fleming, 1984). Acidity is contributed by unsaturated Al^{3+} ions, protonated hydroxyls, and acidic hydroxyls. The basicity is contributed by O^{2-} anion vacancies and basic hydroxyls.

2.1.4 The α-Aluminas

α-alumina trihydrate ($Al_2O_3 \cdot 3H_2O$) in its natural state is termed gibbsite or hydrargillite (Papee and Tertian, 1963). α-alumina trihydrate can be produced in the laboratory by means of the Bayer process. α-alumina trihydrate consists of double layers of hydroxide ions with 2/3 of the intercises occupied by aluminum ions and the hydroxyls are situated opposite each other (Pearson, *et al*, 1992). Particles of α-alumina trihydrate are spherical shaped grains measuring 50 to 100 microns in size (Papee and Tertian, 1963). The α-alumina trihydrates begin to lose their water molecules at approximately 140°C.

α-alumina monohydrate ($Al_2O_3 \cdot H_2O$) is commomly known as beohmite (Pearson, *et al,* 1992). Monohydrate aluminas are obtained from the trihydrates by the use of water or steam at high temperatures (Papee and Tertian, 1963). α-alumina monohydrate consists of double layers in which the oxygen atoms exhibit cubic packing. The hydroxyl ions of one double layer are located over the depressions between hydroxide ions in the adjacent layer such that the double layers are linked by hydrogen bonds between hydroxyls (Pearson *et al*, 1992). Stability of the monohydrates lies in ranges between 140°C – 375°C at pressures less than 140 kg/cm^2 (Papee and Tertian, 1963). α-monohydrates are hexagonal shaped crystals that measure from a few microns to several tens of microns in diameter.

α-alumina (Al_2O_3) is produced when hydrated aluminas or γ-alumina is heated for several hours at a temperature of 1250°C or higher and is free of other crystalline alumina phases (Edwards and Bayha, 1947). α-aluminas are not good adsorbents due to

dehydroxylation and low surface area (Goodboy and Fleming, 1984). α-aluminas have several uses including bedding material in the heat treatment of special alloy steels, a fluxing medium in the melting of steels, a constituent of special china glazes, and as a raw material for the manufacture of dental porcelains. α-aluminas also exhibit the capability to adsorb halides, water, and inorganic acids due to a greater Lewis acidity per surface area than other aluminas . α-aluminas make excellent abrasives due to high mechanical hardness and strength (Edwards and Bayha, 1947).

Figure 2.1: α-alumina trihydrate (X 20,000) (from Papee and Tertian, 1963)

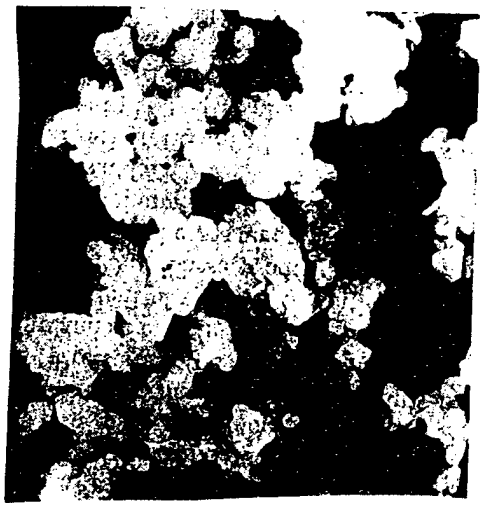

Figure 2.2: α-alumina monohydrate (X 20,000) (from Papee and Tertian, 1963)

2.1.5 The β-Aluminas

β-alumina trihydrate ($Al_2O_3 \cdot 3H_2O$) is termed bayerite in its natural state. It is not a product of the Bayer process. β-alumina trihydrate can be formed by precipitation at room temperature in the pH range of 10 to 13 (Papee and Tertian, 1963). β-alumina trihydrates consists of double layers of hydroxides with the hydroxyl groups of one layer resting in the depressions between the hydroxide positions (Pearson, *et al,* 1992). The β-alumina trihydrates begin to lose their water molecules at 140°C (Papee and Tertian, 1963).

β-alumina monohydrate ($Al_2O_3 \cdot H_2O$), or diaspore, consists of oxygen atoms joined to each adjacent oxygen by way of a hydrogen ion and arranged in hexagonal close packing (Pearson, *et al,* 1992). β-monohydrates are chemically stable in a range of temperatures

from 275°C to 425°C at pressures that exceed 140 kg/cm^2 and are typically 1 to 2 mm in size (Papee and Tertian, 1963).

β-aluminas ($Na_2O \cdot 11Al_2O_3$) are formed only in the presences of alkali (Edwards and Bayha, 1947). β-aluminas consist of alkali-substituted aluminates and related compounds. β-aluminas have received attention for their adsorptive properties with the most common compound being beta sodium aluminate (Goodboy and Fleming, 1984).

2.1.6 The Transition Aluminas

Transition aluminas are a group of Al_2O_3 compounds that lie between the amorphous and crystalline forms. Transition alumina formation is due to the thermal decomposition of alumina before the presence of nearly pure crystalline α-alumina forms at temperatures above 1100°C (Papee and Tertian, 1963). Transition aluminas are divided into six major categories based on temperatures of formation. The well crystallized forms kappa (κ), theta (θ), and delta (δ) which are formed at temperatures above 800°C and the poorly crystallized chi (χ), eta (η), and gamma (γ) make up the other major configurations of transition aluminas.

γ-aluminas' crystalline configuration is cubic shape with a surface area of 400m^2/g to 450 m^2/g and contains mainly localized pores of diameters less than 40 Å (Papee and Tertian, 1963). The γ-alumina has a defect spinel structure in which the oxygens are closely packed in a cubic structure (Goodboy and Fleming, 1984). The oxygen sublattice is well organized, while the aluminum sublattice is random. γ-aluminas form at around 300°C to 400°C from monohydrates (Papee and Tertian, 1963).

The poorly crystallized transition aluminas are obtained from certain amorphous aluminas (see Figure 2.3). The χ-transition alumina is formed from α-trihydrates; η-transition alumina is formed from β-trihydrates; and γ-transition alumina is formed from α-monohydrates (Papee and Tertian, 1963). Transition alumina manufacture begins with the alumina trihydrates in the form of large crystal aggregates. Dehydration occurs via heating, leading to the loss of water molecules and to the formation of α-monohydrate. The solid formation reaches a certain porosity and the formation of α-monohydrate ceases. Untreated trihydrate is used in the production of χ and η transition aluminas (Papee and Tertian, 1963). The α, η, and γ aluminas' specific surface areas decrease as the temperature increases. As the more highly ordered transition aluminas, κ, θ, and δ, are formed with increasing temperature, they exhibit very low surface areas which is less than tens of m^2/g (Papee and Tertian, 1963).

Figure 2.3: Thermal and Hydrothermal Transformations of Alumina

(from Papee and Tertian, 1963)

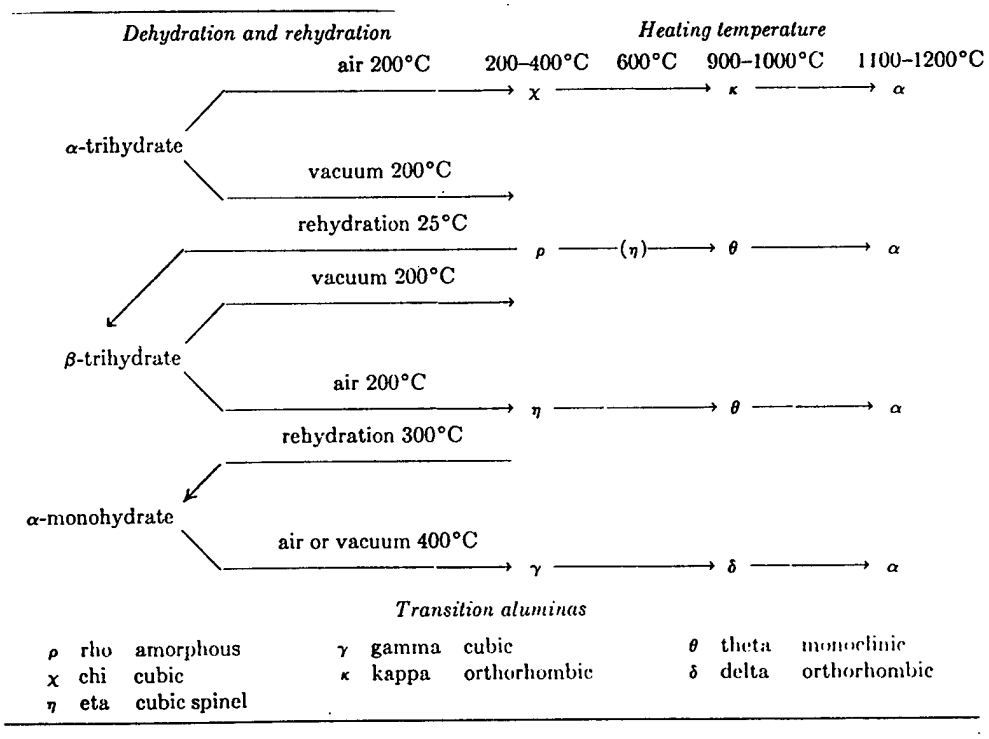

2.1.7 Alumina Gels

Alumina gels refer to preparations of alumina which are amorphous, or mainly amorphous, hydrated forms of alumina (Papee and Tertian, 1963). Alumina gels crystallize upon aging (Pearson, *et al*, 1992). Alumina gels are formed by adding ammonia or alkali to a solution of a salt such as ammonium chloride (Edwards and Bayha, 1947). Alumina gels also contain excess water, sometimes as much as 5 moles H_2O/ mole Al_2O_3 even after dehydration (Pearson, *et al,* 1992). These gels are formed by the hydrolysis of organoaluminum compounds, such as aluminum alkoxides (Pearson, *et al*; 1992). The two major alumina constituents of the gels are amorphous phase and colloidal boehmite (Papee and Tertian, 1963). These two phases normally coexist with the addition of crystallized trihydrates. The physical characteristics of alumina gels are dependent upon the pH at which precipitation occurs. When precipitation occurs at pH less than 7.0, the gel is amorphous with many impurities. The impurities lead to an increase in active pore sites and an increased capability of retaining a large amount of ions. Amorphous gels are also present when precipitation occurs up to a pH of about 8.0. At pH values of approximately 9.0, precipitation produces a gel-type boehmite with fewer water molecules per mole of alumina present than for the gels obtained at lower pH. At pH values greater than 10, the alumina gels form finely crystallized hydrates. The crystallization rate for alumina gels is dependent upon the OH^- ion concentration and temperature. The rate increases with an increase in pH, temperature and age (Pearson, *et al*, 1992).

Gelatinous boehmite, commercially known as alumina gel, is used in the preparation of adsorbents, desiccants, catalysts, and pharmaceutical materials (Pearson, *et al*, 1992).

Alumina gels are dehydrated by heating at high temperatures. Heating also activates the dehydrated aluminas' surface, producing particles with high surface area (Edwards and Bayha, 1947). These high surface area particles make outstanding adsorbents and catalyst supports.

Figure 2.4: Classification of Alumina Hydroxides (Pearson, *et al*, 1992)

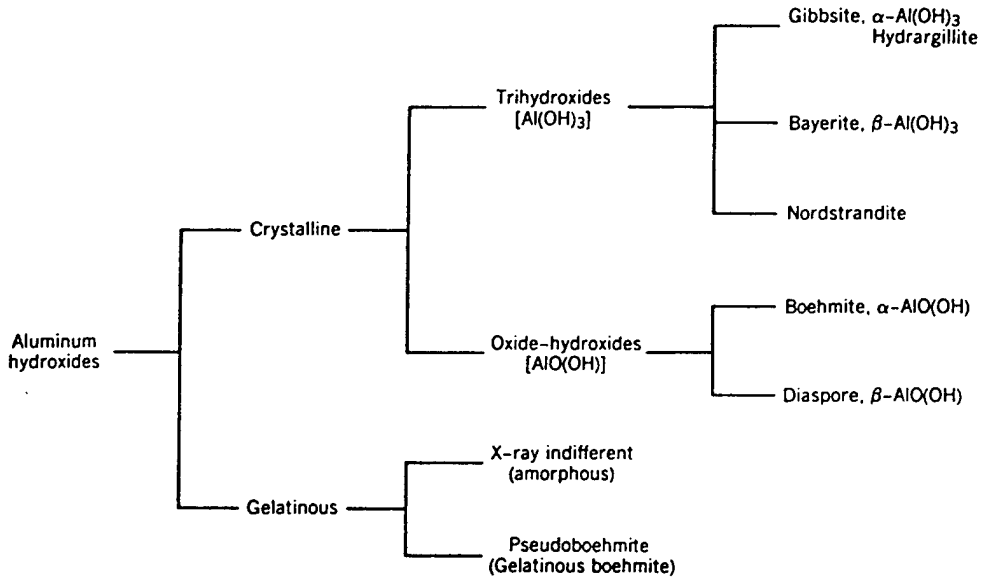

2.1.8 Availability and Alumina Safety

The alumina industry has grown over the past thirty years both within the United States and globally. The world consumption of bauxite (except in USSR and China) was 20 million tons in 1963 (Papee and Tertian, 1963). The world aluminum hydroxide production in 1988 had risen to 50 million tons by 1988 (Pearson, *et al*, 1992). In the United States 600,000 metric tons of aluminum oxide was used in 1988 for chemical purposes. The various chemical applications were 40% used as fillers, 45% used as aluminum chemicals, and 15% used for other reasons. In 1985, the United States production of activated alumina was listed as 10,000 tons per year. This number grew to 50,000 tons per year by 1990. The major North American producers of aluminum oxide products include Alcoa, La Roche, Discovery, and Alcan.

Bayer process aluminum products listed in 1989 include α aluminum trihydroxide for \$0.26/kg – \$0.75/kg, tabular alumina for \$0.86/kg - \$1.06/kg, and the activated aluminas costs from \$0.60/kg - \$3.00/kg (Pearson, *et al*, 1992).

Aluminum oxide is nonflammable and nontoxic. The fine mesh alumina particles can cause eye irritation (Pearson, *et al*, 1992). Studies conducted on factory workers at alumina refining industries have failed to show that aluminum hydroxide collects in human lungs. Aluminum hydroxide could cause death by ingestion only if a sufficient amount were consumed to cause intestinal blockage rather than by toxicity.

2.2 LEAD CHEMISTRY

2.2.1 Background

The oxidation states of lead are 0, +2, +4. The most common and most complex hydrolysis behavior is Pb^{+2} (Baes and Mesmer, 1976). Pb_3O_4 and PbO_2 are two other fairly common forms of lead which occur in very oxidizing environments. Baes and Mesmer (1976) present a rigorous evaluation of the chemistry of lead in their text and will be followed closely through this section. Baes and Mesmer report from phase diagrams by Stumm and Morgan (1970) that PbO_2 produces Pb^{2+} and O_2 below a neutral pH with PbO_2 and Pb_3O_4 showing very narrow ranges of stability.

2.2.2 Lead (II) Species

The mononuclear form of lead (PbO) occurs in two crystalline forms and a hydrated form (Baes and Mesmer, 1976). The mononuclear crystalline forms are litharge (red) which is a stable form and massicot (yellow). The hydrated form of PbO has been reported with two different compositions. Pleisner (1907) identified $2PbO{\cdot}H_20$ and Todd and Parry (1964) found $2.5PbO{\cdot}H_2O$. The solubility constant which was calculated from the free energy data of the National Bureau of Standards (NBS, 1968) compilation for the red PbO at a temperature of 25°C:

$$PbO(s) + 2H^+ \rightarrow \quad Pb^{2+} + H_2O \qquad \log K_s = 12.72$$

The lead (II) species which are formed in alkaline solutions are mononuclear .

The polynuclear forms of Pb(II) exist as $Pb_3(OH)_4^{2+}$, $Pb_4(OH)_4^{4+}$, and $Pb_6(OH)_8^{4+}$. The $Pb_4(OH)_4^{4+}$ species is the most definitive species while the $Pb_3(OH)_4^{2+}$ is the least

prevelent. The species Pb_2OH^{3+} is another polynuclear lead (II) species that is considered rare because it only appears in certain experimental conditions. The enthalpy and entropy of the polynuclear lead (II) species as reported by Carell and Olin (1962) are given in Tables 2.1 and 2.2.

Table 2.1 Enthalpy of Pb(II) hydrolysis equilibria in 3M $NaClO_4$ at 25°C

Species		ΔH (kcal/mole)
$4\ Pb^{2+} + 4H_2O \rightarrow$	$Pb_4(OH)_4^{4+} + 4H^+$	20.07±0.12
$6\ Pb^{2+} + 8H_2O \rightarrow$	$Pb_6(OH)_8^{4+} + 8H^+$	49.44±0.08
$3\ Pb^{2+} + 4H_2O \rightarrow$	$Pb_3(OH)_4^{2+} + 4H^+$	26.5±0.8

Table 2.2 Entropy of Pb(II) hydrolysis equilibria in 3M $NaClO_4$ at 25°C

Species		ΔH (kcal/mole)
$4\ Pb^{2+} + 4H_2O \rightarrow$	$Pb_4(OH)_4^{4+} + 4H^+$	-20.8±0.8
$6\ Pb^{2+} + 8H_2O \rightarrow$	$Pb_6(OH)_8^{4+} + 8H^+$	-27.0±3.1
$3\ Pb^{2+} + 4H_2O \rightarrow$	$Pb_3(OH)_4^{2+} + 4H^+$	-15.8±3.8

Using ultracentrifuge and light scattering measurements , Esval and Johnson (1965) found that at a hydroxyl number, *n*, of about 1.0, the degree of polymerization is 4, and it was increased further in more basic solutions where the supporting electrolyte was 1M $NaClO_4$. In x-ray diffraction studies performed by Johansson and Olin (1968), the

structural information of tetranuclear, $Pb_4(OH)_4^{4+}$, and hexanuclear, $Pb_6(OH)_8^{4+}$, was determined. These studies were possible because at lead(II) concentrations of 1.6M and *n* of 1.33, the predominant species was $Pb_6(OH)_8^{4+}$; and at lead(II) concentrations of 5.0M and *n* of 1.0, the predominant species was $Pb_4(OH)_4^{4+}$. At *n* of 1.0, each of the lead atoms had three closest atomic neighbors, all at 3.85Å (Baes and Mesmer, 1976). This equidistant measurement causes the molecule formation to be tetrahedral. The work of Maroni and Spiro (1967) also confirm this tetrahedral formation with Raman spectral studies on similar solutions.

Figure 2.5: Structure of $Pb_4(OH)_4^{4+}$ Molecule from x-ray Diffraction

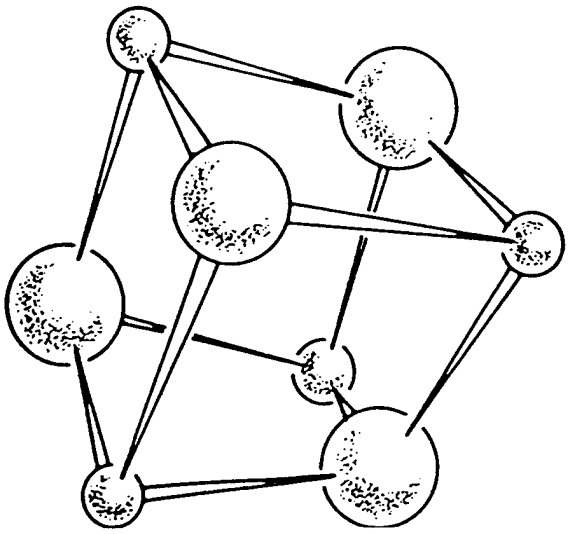

At *n* of 1.33, the peak of 3.85Å is broadened and has 35% greater area with the average of the closest atomic neighbors approximately 4 Å. The distances between the atoms are not equal and two more peaks appear at 6.4 Å and 7.1 Å with considerably lower area .

2.2.3 Lead (IV) Species

The lead(IV) species information is not known with much reliability. Some equilibria data has been reported by Vanyukova *et al.*(1962) by the following reactions:

$$PbO_2(s) + H_2O + H^+ \rightarrow \quad Pb(OH)_3^+ \qquad \text{Log } K_s \approx -4.8 \qquad \textbf{(2.1)}$$

$$PbO_2(s) + 2H_2O + H^+ \rightarrow \quad Pb(OH)_4 \qquad \text{Log } K_s \approx -4 \qquad \textbf{(2.2)}$$

occurring in concentrated sulfuric acid solutions.

2.2.4 Organic Lead Species

Organic lead species are also known as lead alkyls or methyl-lead. Organic leads were used as antiknock agents in gasoline, and large amounts of these alkyls reach the atmosphere through evaporation and combustion (Baes and Mesmer, 1976). Methyl leads are so toxic they have been removed from all gasolines. Methyl-butyl test ether is now used in antiknock agents. Freidline and Tobias (1966) investigated the hydrolysis of $(CH_3)_2Pb^{2+}$ (dimethyllead ion) in 3M $NaClO_4$ media. The observed species were $(CH_3)_2Pb(OH)_2$, $(CH_3)_2Pb(OH)_3^-$, $[(CH_3)_2Pb]_2(OH)_2$, and $[(CH_3)_2Pb]_3(OH)_4^{2+}$. The equilibrium quotients found from Freidline and Tobias are listed in Table 2.3.

Table 2.3: $(CH_3)_2Pb^{2+}$ hydrolysis at 25°C in 3M $NaClO_4$

Species	Log Q
$(CH_3)_2PbOH^+$	<-7.4
$(CH_3)_2Pb(OH)_2$	-15.543
$(CH_3)_2Pb(OH)_3^-$	-28.52
$[(CH_3)_2Pb]_2(OH)_2^{2+}$	-10.827
$[(CH_3)_2Pb]_3(OH)_4^{2+}$	-24.31

Freidline and Tobias used Raman spectra to determine that $(CH_3)_2Pb^{2+}$ had a linear molecular skeleton with weak covalent interactions between the lead alkyl ion and the

hydrate water molecules and nitrate ions in the first coordination sphere (Baes and Mesmer, 1976).

2.2.4 Lead Speciation in Freshwater

Mass balances for Pb(II) in fresh water given by Stumm and Morgan (1996)

$$Pb(II)_T = [Pb^{2+}] + \Sigma[Pb(OH)_i] + \Sigma[Pb(CO_3)_i] + \Sigma[Pb(SO_4)_i] + \Sigma[Pb(Cl)_i], \text{ and}$$

$$Pb(II)_T = [Pb^{2+}] (1 + \Sigma \beta_{i,OH}[OH^-]^i + \Sigma \beta_{i,CO3}[CO_3^{2-}]^i + \Sigma \beta_{i,SO4}[SO_4^{2-}]^i$$

$$+\Sigma\beta_{i,Cl}[Cl^-]^i). \qquad \textbf{(2.3)}$$

In reviewing the aqueous lead equilibrium models, all relevant reactions must be taken into account. There are two primary reactive lead systems to consider, the Pb-H_2O system and the Pb-H_20-CO_2 system.

For the Pb-H_2O systems, the following equilibrium reactions are of interest (Stumm and Morgan, 1970).

$$PbO_2(s) + 4H^+ + 2e^- = 2H_2O + Pb^{2+} \qquad \log K = 49.2 \qquad \textbf{(2.4)}$$

$$Pb^{2+} + 2e^- = Pb(s) \qquad \log K = -4.26 \qquad \textbf{(2.5)}$$

$$PbO(s) + 2H^+ = Pb^{2+} + H_2O \qquad \log K = 12.7 \qquad \textbf{(2.6)}$$

$$PbO(s) + 2H_2O = Pb(OH)_3^- + H^+ \qquad \log K = -15.4 \qquad \textbf{(2.7)}$$

Figure 2.6 pE-pH diagram for Pb-H_2O System

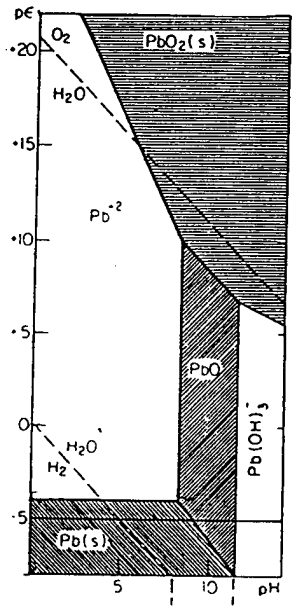

Figure 2.7 pC – pH Diagram for Pb-H_2O System

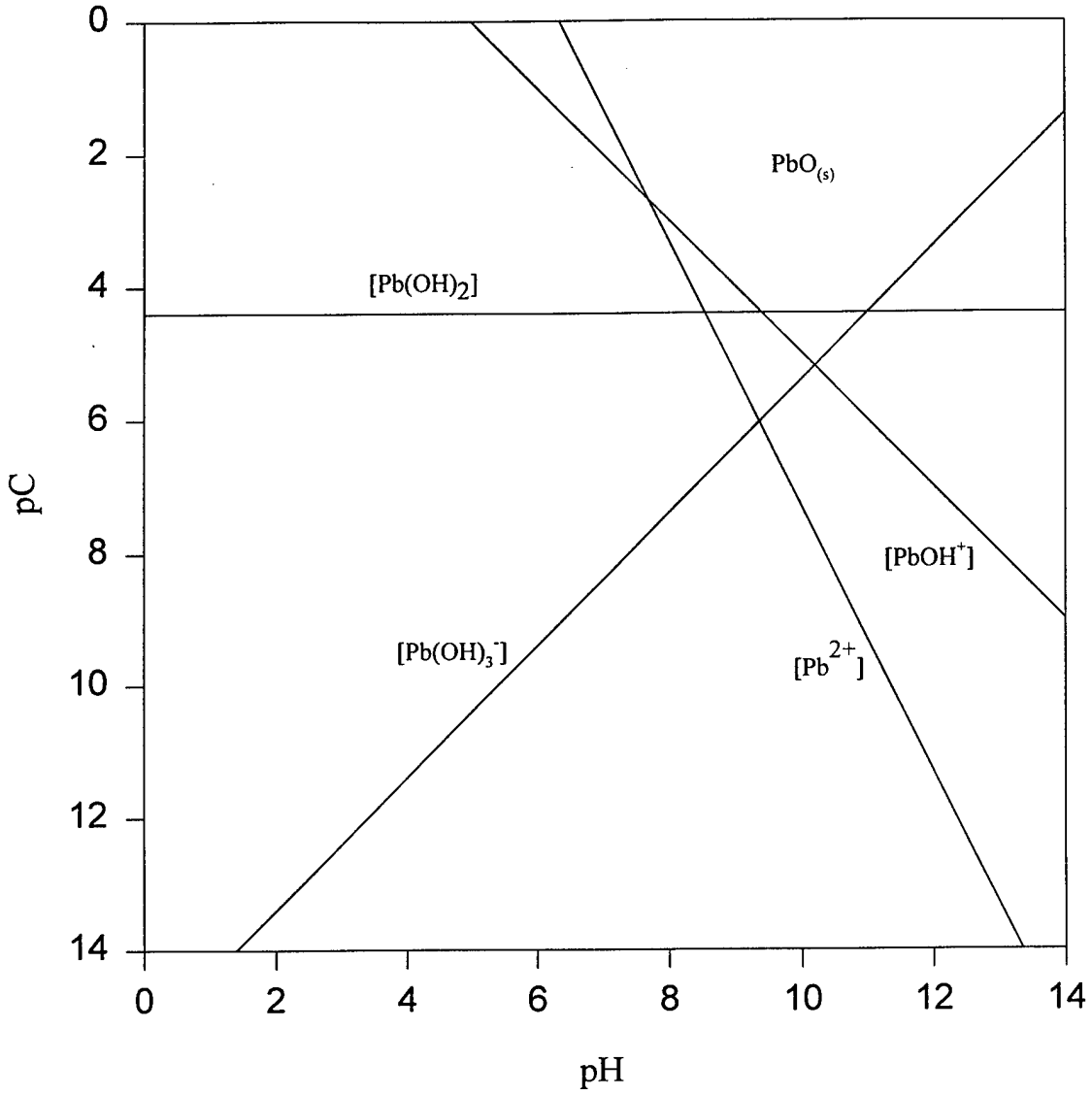

The pE versus pH diagram in Figure 2.6 was formed from Equations (2.4) to (2.7) and show that elemental lead dissolves at low pH, $PbO_2(s)$ is unstable in acidic solutions, and soluble Pb^{2+} cannot exist at appreciable concentrations of near or slightly alkaline.

For the Pb-H_2O-CO_2 systems, the following equations in addition to the Pb-H_2O equations are important (Stumm and Morgan, 1970).

$$PbCO_3(s) = Pb^{2+} + CO_3^{2-} \qquad \log K = -12.83 \quad \textbf{(2.8)}$$

$$Pb(CO_3)_2(OH)_2(s) + 2H^+ = 3Pb^{2+} + CO_3^{2-} + 2H_2O \qquad \log K = -18.8 \quad \textbf{(2.9)}$$

Figure 2.8 pE-pH diagram for Pb-H_2O-CO_2 System

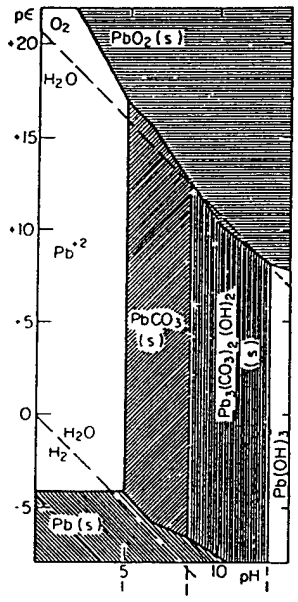

2.3 SORPTION MODELS

2.3.1 Background

Sorption models are used to represent the behavior between ions and surfaces for particles in solution. Liming He (1995) presented a comprehensive evaluation of sorption theory and equilibrium models. There are two main categories of models used to describe sorption at equilibrium. These two categories are surface isotherms and complexation models. The surface isotherms have been used to describe the partitioning of solutes between solid and aqueous phases. Surface complexation models have mainly been used by scientists in developing an understanding of the coordinative properties of mineral surface functional groups.

2.2.2 The Langmuir Isotherm

The Langmuir isotherm is the most common adsorption model (Clark, 1996). The Langmuir equation is expressed as:

$$q_e = \frac{Q^o bC_e}{1 + bC_e} \qquad \textbf{(2.10)}$$

where;

q_e = number of moles (sometimes mass) of adsorbate adsorbed per unit mass of adsorbent

Q^o = number of moles (sometimes mass) of adsorbate adsorbed per unit mass of adsorbent at complete surface coverage

b = coefficient related to the adsorption energy.

C_e = equilibrium solute concentration

Linearizing equation (2.10) produces the following equation

$$\frac{1}{q_e} = (\frac{1}{Q^0 b})(\frac{1}{C_e}) + \frac{1}{Q^o} \qquad \textbf{(2.11)}$$

The values for Q^o and b may be determined by plotting *1/qe* vs. *1/Ce*. The slope of this linear plot is equal to $1/Q^o b$ and the y-intercept is equal to $1/Q^o$. In liquid-liquid systems, Q^o and b are determined for a specific adsorbent and adsorbate and are generally a function of temperature , pH, and ionic strength (Clark, 1996). The coefficient, b, which is related to the adsorption energy may be calculated by (Adamson, 1990):

$$b = \frac{N_o \sigma^o \tau_o}{(2\Pi MRT)^{1/2}} \exp(Q/RT) \qquad \textbf{(2.12)}$$

where;

N_o = Avogadro's number (6.02×10^{23} ions mol^{-1})

σ^o = area of adsorptive site, cm^2

τ_o = time the ion can stay on the surface, sec.

M = weight of adsorbed ion, g

R = gas constant (8.314×10^7 ergs $deg^{-1}mol^{-1}$)

T = absolute temperature

Q = adsorption energy, erg mol^{-1}

The Langmuir isotherm is based on several assumptions which are as follows (Clark, 1996):

1. The Langmuir model assumes physiosortion of a monolayer.
2. In liquid or gas phase, the adsorbate behaves as an ideal gas or solute. The accuracy of this assumption is unknown because of the complexity and large size of organic molecules. The lower the solute concentration , the more accurate is this assumption.
3. Adsorbate molecules remain at specific adsorption sites. This is accurate for chemisorption, but physisorbed molecules tend to diffuse along adsorbate surfaces.
4. Adsorption sites are uniformly distributed on the adsorbent surface, and the energy of interaction of each adsorption site is the same. Many adsorbing surfaces have heterogeneous adsorbing surfaces with different interaction energies.
5. There are no interactions between adsorbed molecules. Molecular interaction may occur due to electrostatic, van der Waals, and other forces.

The Langmuir isotherm typically forms a close fit, linear plot for low solute concentrations. However, at high solute concentrations, a non-linear relationship between $1/q_e$ and $1/C_e$ develops. The non-linear behavior points to the fact that the adsorption energy is not constant, but a function of adsorption with no defined maximum (Sanyal and Datta, 1991). Several modifications can be made to the Langmuir isotherm to account for the nonlinearity (He, 1995).

Syers *et al.* (1973), Ram *et al.*(1987), and Mehadi and Taylor (1988) produced experimental data that describes a two-site Langmuir isotherm. The two-site isotherm is written as,

$$q_e = \frac{Q_1^o b_1 C_e}{1 + b_1 C_e} + \frac{Q_2^o b_2 C_e}{1 + b_2 C_e} \qquad \textbf{(2.13)}$$

The two-site Langmuir isotherm attempts to account for the problem of heterogeneous adsorbing surfaces (White and Zelazny, 1986). Equation (2.13) can be attributed to the variable energy of adsorption of aqueous ions by soils (Posner and Bowden, 1980).

Another modification to the Langmuir equation was presented by Sibbeson (1981) as follows,

$$q_e = \frac{Q^o b C_e^{-D} C_2}{1 + b C_e^{-D} C_2} \qquad \textbf{(2.14)}$$

Where D is a coefficient. Equation (2.14) shows that adsorption energy decreases with increasing ion concentration.

2.3.3 The Freundlich Isotherm

The Freundlich isotherm is an empirical relationship that is expressed as

$$q_e = K_f C e^{1/n} \qquad \textbf{(2.15)}$$

where;

K_f = empirical constant related to the capacity of adsorbent material to adsorb the adsorbate (higher K_f value, more material potentially adsorbed).

n = empirical constant related to the affinity of the adsorbate for the surface (smaller n value, greater the affinity of the adsorbate to bind to the surface).

Linearizing equation (2.15) leads to the following equation.

$$log\ q_e = log\ K_f + 1/n\ log\ C_e \qquad \textbf{(2.16)}$$

The values for K_f and n may be determined by plotting log q_e versus log C_e. The slope of this line equals to $1/n$, and the y-intercept equals K_f. He (1995) states there is a high degree of correlation between the Freundlich K_f, Langmuir Q^o, and the Temkin adsorption parameter. Less emphasis is attached to the Freundlich equation because it does not provide any measure of an adsorption maximum.

One error that occurs with the Freundlich equation is that ions may be attached to particles before adsorption of free, aqueous phase ions occurs (Barrow, 1978). Barrow provided an equation to account for the initial presence of these ions in the model as follows,

$$q_e = K_f C_e^{\ 1/n} - Q_n \qquad \textbf{(2.17)}$$

2.3.4 The Temkin Isotherm

The Temkin isotherm is based upon the assumption that the bonding energy of adsorption decreases linearly with increasing surface coverage (He, 1995). For a wide range of concentrations, the Temkin isotherm is quite complex, but for the middle range of surface coverage, the equation reads,

$$\frac{q_e}{q_m} = \frac{RT}{b} \ln(AC_{eq}) \qquad \textbf{(2.18)}$$

where A and b are empirical coefficients.

The Temkin equation can be simplified to the following equation:

$$q_e = \beta \, lnC_{eq} + B \qquad \textbf{(2.19)}$$

where β and B are coefficients of adsorption. The values for β and B can be determined by plotting q_e versus ln C_e. The slope of the line equals β, and the y-intercept equals B. The Temkin equation should plot as a straight line, however, plots for soils using the Temkin equation generally yield a slight curve (Fox and Kamprath, 1970; Roy and DeDatta, 1985; Russell *et al.*, 1988). He (1995) found that the data from sorption studies using the Temkin plots were better than the Langmuir isotherm plots over a broader range of concentrations.

2.3.4 Surface Complexation Models

Surface complexation models extend the double-layer theory of Debye-Huckle or Gouy-Chapman to account for increased ion concentration near the surface of colloids (He, 1995). Surface complexation models are based on mass balances, mass action,

charge balances, and charge-potential relationship equations. Differences in surface complexation models occur due to the treatment of their interfacial structure, including the number of adsorption planes and types of surface complexes. Several assumptions are made for the development of the surface complexation models. These assumptions include (He, 1995)

1. The surface is composed of specific functional groups that react with dissolved solutes to form surface complexes (ion pairs or coordinative complexes) in a manner analogous to complexation reactions in a homogenous solution.
2. Equilibria of surface complexation and ionization can be described by mass law balances. Equilibrium constants for the surface reactions (K) differ from those in the aqueous phase in that they are modified by a correction term for the electrostatic energy of the interface (*edl*) that effectively represents an activity coefficient ratio for the surface species (Goldberg, 1992)

$$K = K_c \cdot edl \qquad \textbf{(2.20)}$$

Where;

K = the conditional equilibrium constant written in terms of activities of aqueous species and concentrations of surface species.

edl = model-dependent term involving the surface potential or potential within adsorption planes.

3. Surface charge and surface charge potential are treated as necessary consequences of chemical reactions of the surface functional groups. The Gouy-Chapman electric double layer theory is appropriate for diffuse layer charge and potential surrounding a colloidal particle.

4. The apparent bonding constants determined for the mass action equations are empirical parameters related to thermodynamic constants via the rational activity coefficients of the surface species.
5. Adsorption is limited to specific planes; the average charge of a plane is determined by mass balance equations for each plane and the charge of the species in that plane. The sum of the charge of all adsorption planes and the diffuse layer charge is zero according to the law of electroneutrality.

2.3.5 The Constant Capacitance Model

The constant capacitance model was developed by Hohl and Stumm (1976) and subsequently improved by Sposito (1984), Hayes (1987), Davis and Kent (1990), and Goldberg (1992). The constant capacitance model has only one plane (see Figure 2.8). Assumptions of the constant capacitance models are as follows (He, 1995):

1. The surface is composed of amphoteric surface sites.
2. There is only one plane in the interfacial region: a surface plane for adsorption of H^+ and OH^-, and all other specifically adsorbed solutes.
3. Ionic strength effects are ignored, thus background electrolyte ions are not taken into account.
4. The charge-potential relationship is written as:

$$\sigma_o = C\ \psi_o \qquad \textbf{(2.21)}$$

where,

σ_o = surface charge density

C = capacitance of the mineral-water

ψ_o = constant medium reference state used for aqueous species; a zero charge reference state is used for surface species.

Figure 2.9: Constant Capacitance Model (from He, 1995)

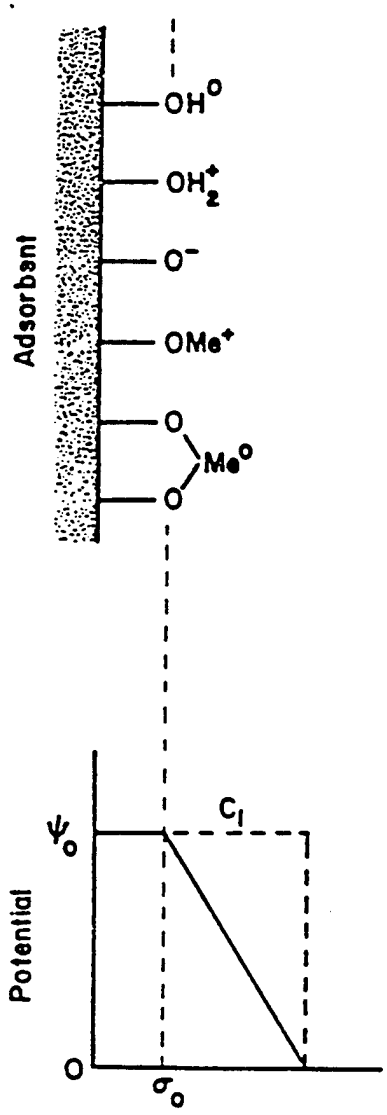

Equations for the general surface complexation reactions are as follows (Goldberg, 1992):

$$XOH + H^+ \rightarrow XOH_2^+ \quad \textbf{(2.22)}$$

$$XOH \rightarrow XO^- + H^+ \quad \textbf{(2.23)}$$

$$XOH + M^{m+} \rightarrow XOM^{(m-1)} + H^+ \quad \textbf{(2.24)}$$

$$2\,XOH + M^{m+} \rightarrow (XO)_2 M^{(m-2)} + 2H^+ \quad \textbf{(2.25)}$$

$$XOH + L^{l-} \rightarrow X_2 L^{(l-1)-} + OH^- \quad \textbf{(2.26)}$$

$$2\,XOH + L^{l-} \rightarrow X_2 L^{(l-2)-} + 2\,OH^- \quad \textbf{(2.27)}$$

where;

XOH = surface functional groups

M = metal ion

$m+$ = charge on the metal ion

L = ligand

$l-$ = charge on the ligand

The intrinsic equilibrium constants used to describe these reactions are (Goldberg, 1992),

$$K^+ = \frac{[XOH_2^+]}{[XOH][H^+]} \exp\left(\frac{F\Psi}{RT}\right) \quad \textbf{(2.29)}$$

$$K^- = \frac{[XO^-][H^+]}{[XOH]} \exp\left(-\frac{F\Psi}{RT}\right) \quad \textbf{(3.30)}$$

$$K_M^1 = \frac{[XOM^{(m-1)}][H^+]}{[XOH][M^{m+}]} \exp\left(\frac{(m-1)F\Psi}{RT}\right) \quad \textbf{(3.31)}$$

$$K_M^2 = \frac{\left[(XO)_2 M^{(m-2)}\right]\left[H^+\right]^2}{\left[XOH\right]^2\left[M^{m+}\right]} \exp\left(\frac{(m-2)F\Psi}{RT}\right) \qquad \textbf{(3.32)}$$

$$K_L^1 = \frac{\left[XL^{(l-1)}\right]\left[OH^-\right]}{\left[XOH\right]\left[L^{l-}\right]} \exp\left(-\frac{(l-1)F\Psi}{RT}\right) \qquad \textbf{(3.33)}$$

$$K_L^2 = \frac{\left[X_2 L^{(l-2)}\right]\left[OH^-\right]^2}{\left[XOH\right]^2\left[L^{l-}\right]} \exp\left(-\frac{(l-2)F\Psi}{RT}\right) \qquad \textbf{(3.34)}$$

where;

[] = metal ion concentration

To determine this equilibrium problem, the mass balance and the charge balance equations are needed. The mass balance equation for the surface functional group is:

$$[XOH]_T = [XOH] + [XOH_2^+] + [XO^-] + [XOM^{(m-1)}] + [(XO)_2M^{(m-2)}] + [XL^{(l-1)-}] + X_2L^{(l-2)-}], \qquad \textbf{(3.35)}$$

and the charge balance equation is,

$$\sigma = [XOH_2^+] - [XO^-] + (m-1)[XOM^{(m-1)}] + (m-2)[(XO)_2M^{(m-2)}] - (l-1)[XL^{(l-1)-}] - (l-2)[X_2L^{(l-2)-}] \qquad \textbf{(3.36)}$$

The constant capacitance model has been successfully used to describe metal adsorption on silica (Schindler *et al.*, 1976; Osaki *et al.*, 1990a,b), aluminum oxide (Hohl and Stumm, 1976), iron oxide (Lovgren *et al.*, 1990), and kaolonite (Schindler *et al.*, 1987,and Osaki *et al.*, 1990b).

2.3.6 The Diffuse Layer Model

The diffuse layer model was first proposed by Stumm *et al.* (1970). Dzombak and Morel (1990) presented a revised version of the diffuse layer model termed the generalized two-layer model. The diffuse layer model describes reactions that occur with amphoteric hydroxyl groups that form ionized sites (see Figure 2.9). The molecular hypotheses of the diffuse layer model are as follows (He, 1995):

1. There are two planes in the interfacial region, (1) surface plane for adsorption of H^+, OH^-, and all specifically adsorbed ions (2) the diffuse layer representing the closest distance of approach for all counterions.
2. The charge-potential relationship in the diffuse layer is described by the Gouy-Chapman theory:

$$\sigma_d = -(8R\varepsilon\varepsilon_o I x10^3)^{1/2} \sinh(ZF\psi_d/2RT) \qquad \textbf{(3.37)}$$

where;

σ_d = net charge density (C/m^2) in the diffuse layer

ε = dielectric constant (dimensionless)

ε_o = permitivity of free space (8.854×10^{-12} C v^{-1} m^{-1})

I = molar electrolyte concentration

F = Faraday constant

ψ_d = mean potential at start of diffuse layer (Dzombak and Morel, 1990)

3. There are no capacitance parameters required due to the electrical potential at the beginning of the diffuse layer being equal to the surface potential.

4. The infinite reference state is used for aqueous species; a zero surface charge reference state is used for surface species.

The diffuse double layer model has two adjustable parameters which are applied uniformly to low ionic strength solutions, K^+ and K^- (He, 1995). The diffuse layer model depicts ion adsorption on a small set of high-affinity "strong" sites and a large set of low-affinity "weak" sites (Dzombak and Morel, 1990). Sorption for the diffuse layer model which occurs on both types of sites is described by the following reactions,

$$X^sOH + M^{m+} \rightarrow X^sOM^{(m-1)} + H^+ \qquad \textbf{(3.38)}$$

$$X^WOH + M^{m+} \rightarrow X^wOM^{(m-1)} + H^+ \qquad \textbf{(3.39)}$$

where;

s = high-affinity sites

w = low-affinity sites

Figure 2.10: Diffuse Layer Model (from He, 1995)

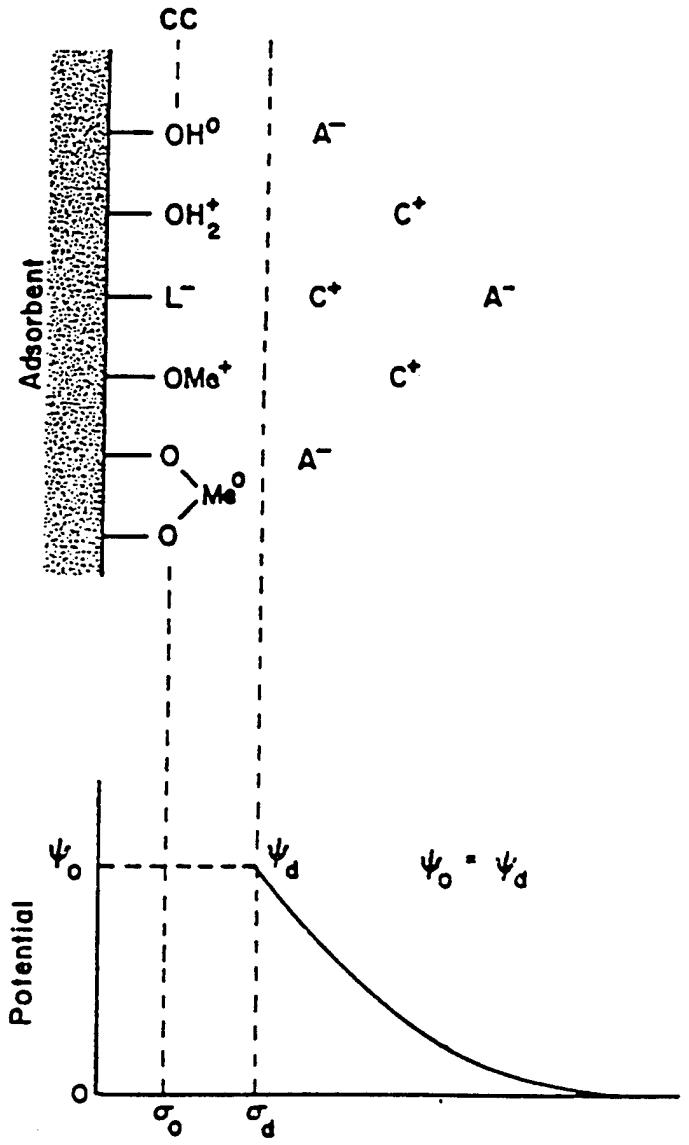

The diffuse layer model has been used to model cadmium adsorption onto polymetric lates (Harding and Healy, 1985a,b) and ferrihydrate (Dzombak and Morel, 1986).

2.3.7 The Triple Layer Model

Since the constant capacitance model and the diffuse layer model describe sorption on only one plane, it is difficult to distinguish between the weakly and strongly binding ions (Hayes, 1987). The basic Stern model was expanded to improve on the inadequacies of the constant capacitance and diffuse layer models by creating a three-plane model for the mercury electrode/aqueous interface (Davis and Kent, 1990). The Stern model contains two adsorption planes; a surface plane (o-plane) for the potential determining ions, and a specific adsorption plane (β-plane) for counterions which bind more weakly (He, 1995). However, the Stern model does not account for the capacitance between the β-plane and the diffuse layer plane. The triple layer model was developed to correct for this error and account for this capacitance (see Figure 2.10) (Yates et al., 1974). The triple layer model has shortcomings due to only the H^+ and OH^- ions forming surface complexes, while all of the other sorbing ions were assumed to be formed in the outer region (Davis *et al.*, 1978). A correction to the original triple layer model was proposed and this revision allowed for the formation of both inner- and outer-sphere complexation (Hayes, 1987).

Figure 2.11: Original Triple Layer Model (from Hayes, 1995)

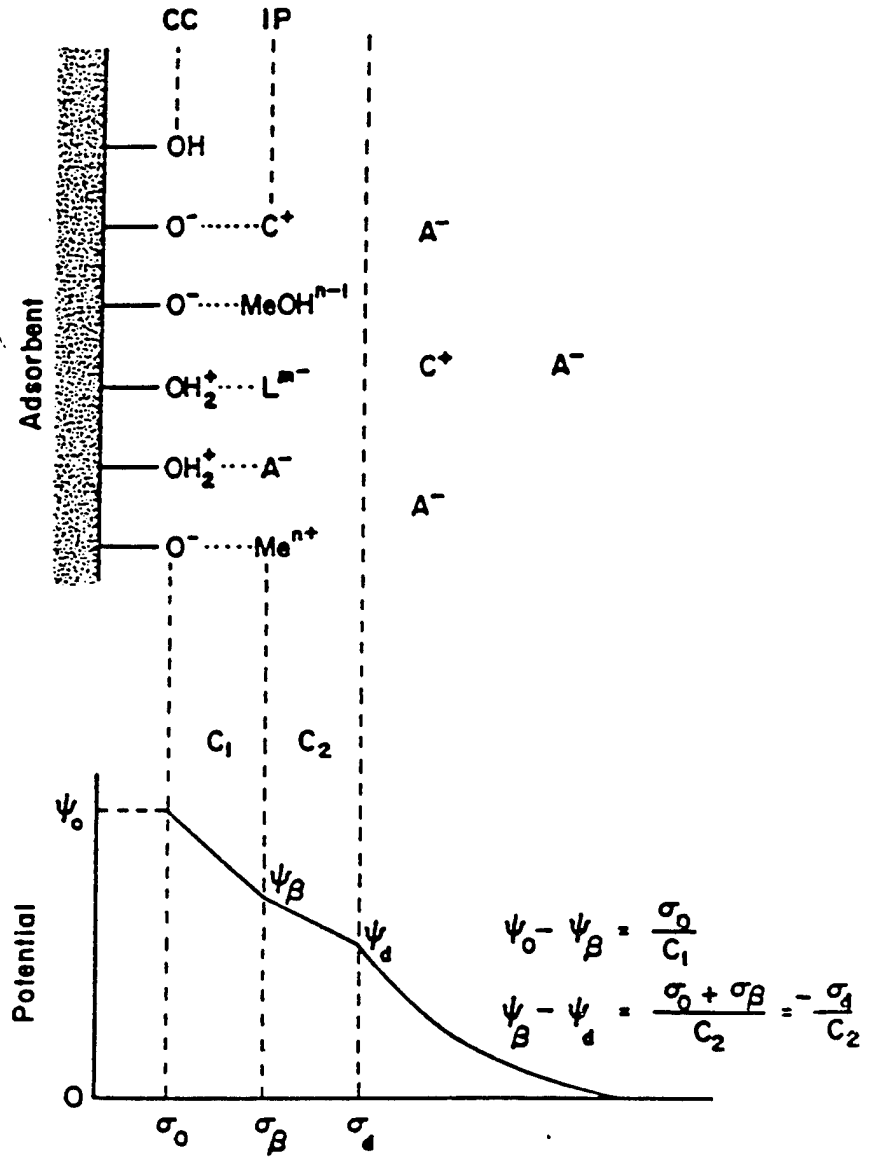

The hypotheses for the triple layer model are as follows (He, 1995):

1. The surface is composed of amphoteric sites.
2. There are three interfacial regions (1) a surface plane (o-plane) for the adsorption of H^+, OH^-, and other strongly-adsorbed ions; (2) a near-surface plane (β-plane) for weakly-adsorbed ions; (3) a diffuse layer plane (d-plane).
3. The Stern-Graham interfacial model is applied for the charge-potential relationships for the two regions between the three layers.

The triple layer model has been used to describe adsorption of metal ions, inorganic anions and organics on oxides, clay minerals, and soils (Goldberg, 1992). The triple layer model has also been used to describe cadmium adsorption on smectites, with an inner-sphere cadmium complexes on aluminum hydroxide edge sites and outer-sphere complexes on silicon hydroxide edge sites (Zachara and Smith, 1994).

2.3.8 The Four layer Model

The four layer model was first proposed by Bowden *et al.* (1977 and 1980) and subsequently applied by Barrow *et al.* (1980, 1981, and 1989) (see Figure 2.11).

Figure 2.12: Four Layer Model (from He, 1995)

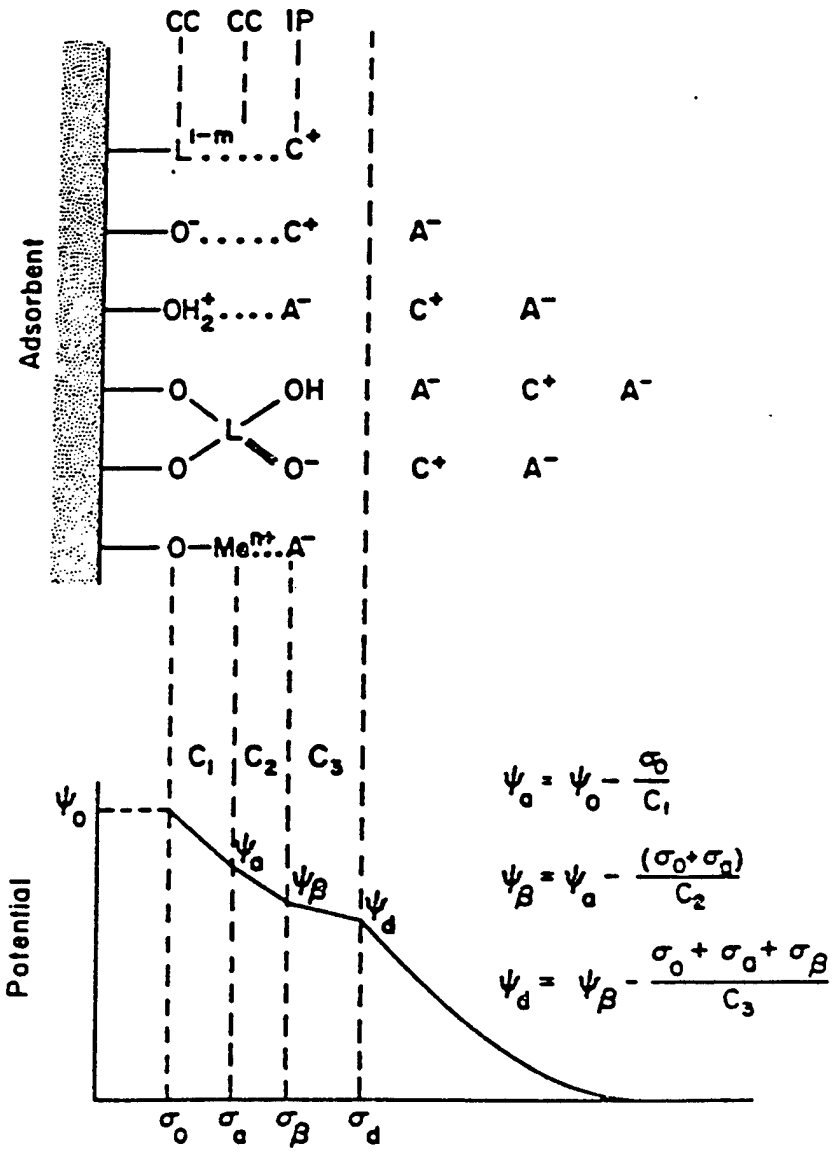

The assumption in developing the four layer model are as follows (He, 1995),

1. The inner-sphere complexes are formed by H^+, OH^-, and other "strongly adsorbed" oxyanions and metals.
2. The H^+ and OH^- ions reside on the surface plane (o-plane).
3. The "strongly adsorbed" ions are placed on the α-plane.
4. The major cations and anions form the outer-sphere complexes and are placed on the β-plane.
5. The fourth plane, the d-plane, is the start of the diffuse layer.

There are four charge-potential equations and charge balance equations to account for the four planes of the four layer model. The charge-potential equations are as follows (Goldberg, 1992)

$$\psi_o - \psi_\alpha = \sigma_o / C_1 \qquad \textbf{(3.40)}$$

$$\psi_\alpha - \psi_\beta = (\sigma_o + \sigma_\alpha) / C_2 \qquad \textbf{(3.41)}$$

$$\psi_\beta - \psi_d = (\sigma_o + \sigma_\alpha + \sigma_\beta) / C_3 = \sigma_d / C_3 \qquad \textbf{(3.42)}$$

The charge balance equations are as follows (Goldberg, 1992):

$$\sigma_o + \sigma_\alpha + \sigma_\beta + \sigma_d = 0 \qquad \textbf{(3.43)}$$

$$\sigma_o = \frac{N_s\left\{K_H\left[H^+\right]\exp(-F\Psi_o/RT) - K_{OH}\left[OH^-\right]\exp(F\Psi_o/RT)\right\}}{1 + K_H\left[H^+\right]\exp(-F\Psi_o/RT) + K_{OH}\left[OH^-\right]\exp(F\Psi_o/RT)} \qquad \textbf{(3.44)}$$

$$\sigma_\alpha = \frac{N_T \sum Z_i K_i a_i \exp(-Z_i F\Psi_o / RT)}{1 + \sum Z_i K_i a_i \exp(-Z_i F\Psi_o / RT)} \quad \textbf{(3.45)}$$

$$\sigma_\beta = \frac{N_s \left\{ K_{cat}\left[C^+\right]\exp(-F\Psi_\beta / RT) - K_{an}\left[A^-\right]\exp(F\Psi_\beta / RT) \right\}}{1 + K_{cat}\left[C^+\right]\exp(-F\Psi_\beta / RT) + K_{an}\left[A^-\right]\exp(F\Psi_\beta / RT)} \quad \textbf{(3.46)}$$

where;

N_s = the maximum surface charge density

N_T = the maximum adsorption of specifically adsorbed ions

K_i = the binding constant

a_i = the activity

Z_i = the charge of the ith specifically adsorbed ion

The adsorption of the metals copper, lead, zinc, nickel, and cadmium on geothite (Barrow et al., 1981, 1989) and zinc on soils (Barrow, 1986) has been represented by the four layer model.

3.0 MATERIALS AND METHODS

3.1 INTRODUCTION

The purpose of this investigation is to determine the effects of pH, alumina particle size, and background matrices on the removal of lead from aqueous solutions. In order to evaluate the performance of lead removal using alumina, the alumina particles and lead solutions had to be prepared. The study was conducted to determine the equilibrium amount and rate of lead sorption using alumina. This chapter reviews the materials and methods used in determining both the equilibrium amount of lead sorbed, and the rate at which lead was removed from aqueous solutions.

3.2 ALUMINUM OXIDE PREPARATIONS

Granular aluminum oxide (γ-alumina) was purchased from Fisher Scientific. The alumina particles were crushed using a mortar and pestal, and separated by size using a series of wire mesh sieves. The particles that accumulated on the >16 screen and the <200 mesh screen (>1190 microns and <74 microns respectively) were retained for equilibrium and kinetic studies.

3.3 LEAD SOLUTIONS PREPARATIONS

Lead solutions were prepared by mixing powdered lead nitrate and distilled, deionized water. The lead solutions were prepared at concentrations of 20 mg/L and 40 mg/l as lead. Competing ions were added to some of the lead solutions with the addition of glacial acetic acid and sodium chloride. Glacial acetic acid was added to one stock solution until the acetic acid concentration reached 1.0 mmole/liter. Granular sodium chloride was added to another stock lead solution to a sodium concentration 0.1 mmole/liter. The pH of all lead solutions were adjusted by the addition of 0.01 mole/liter NaOH and/or 1.0 mole/liter of HCl. NaOH and HCl were added to the solutions using a burette, and the pH was measured using an Orion model 520 A electronic pH meter.

3.4 EQUILIBRIUM PREPARATIONS

The equilibrium study samples were prepared by weighing various masses of alumina, and placing the alumina in 40ml EPA vials (see Table 3.1). The lead solutions, following pH adjustment and addition of background matrices, were added to the EPA vials to a volume of 40 ml of each lead solution. The EPA vials were capped tightly, and subjected to end over end mixing for a period of 7 days. The mixer rotated at a rate so that the alumina particles were dispersed in the solution, but not so fast as to cause a decrease in particle shape and size. The isotherm studies were conducted using lead solutions without background matrices, with 1.0 mmole/liter acetic acid background matrix, and with 0.1 mmole/liter sodium chloride background solution. Also, the isotherms were

prepared using the coarse, >1190 μm alumina particles, and the fine, < 74 μm alumina particles. Finally, the equilibrium tests were run on the lead solutions with pH values in the acidic, neutral, and caustic regions (see Table 3.2). Samples were withdrawn from the vials and filtered using fine mesh Whatman Glass Microfibre Filters (47 mm, Ø Circles) filter paper and acidified with concentrated nitric acid to prevent the precipitation of lead out of solution. The acidified samples were analyzed using a Perkin-Elmer 3110 Atomic Adsorption Spectrophotometer to measure the lead concentration in solution by Standard Methods (APHA, 1998).

Table 3.1: Target Alumina Concentrations for Equilibrium Analysis

Test	Aluminum Concentration (g/L)
1	0.000
2	0.005
3	0.010
4	0.050
5	0.100
6	0.500
7	1.000
8	5.000
9	10.000

Table 3.2: Solution pH Values for Equilibrium Analysis

	Solution pH	
Background Matrix	>1190 μm Mesh	<74 μm Mesh
None	2.75	2.73
	5.17	4.96
	6.81	7.12
	8.06	8.06
1.0 mM Acetic Acid	3.55	3.55
	5.83	5.83
	8.93	8.93
0.1 mM Sodium Chloride	3.20	3.20
	5.57	5.57
	9.15	9.15

3.5 KINETIC PREPARATIONS

The kinetic tests were conducted by combining 1L of the lead solutions with 1 gram of γ-alumina. The solutions were mixed on a magnetic stir plate for the duration of each study. 15 ml samples were withdrawn from the lead and alumina solution over the following time intervals: 0.0, 0.5, 1.0, 2.0, 5.0, 10.0, 15.0, 20.0, 25.0, 30.0, 40.0, 50.0, 60.0, and 120 minutes. Kinetic tests were run using solutions containing only lead and with the background matrices, acetic acid and sodium chloride. The two alumina particle sizes, >1190 μm and <74 μm mesh particle sizes, were examined using each solution. The pH values of the lead solutions ranged from very acidic to very basic depending upon the addition of HCl or NaOH, respectively (see Table 3.3). The withdrawn samples were acidified with concentrated nitric acid to prevent the precipitation of lead in

the solution. The lead concentrations of the samples were then measured using a Perkin-Elmer 3110 Atomic Adsorption Spectrophotometer.

Table 3.3: Solution pH Values for Kinetic Analysis

	Solution pH	
Background Matrix	>1190 µm Mesh	<74 µm Mesh
None	2.57	2.74
	5.34	4.90
	6.50	6.94
	10.20	
1.0 mM Acetic Acid	3.51	3.46
	5.82	5.80
	8.42	8.43
0.1 mM Sodium Chloride	2.58	2.77
	6.98	6.78
	9.57	9.58

4. RESULTS AND DISCUSSION

4.1 INTRODUCTION

The objective of this investigation was to determine the influence of pH, alumina particle size, and the influence of the presence of background matrices on the sorption of lead from aqueous solutions using activated alumina. The influence of these variables was analyzed by determining the percentage of soluble lead removed using equilibrium studies. The influence of these variables was also assessed by determining the rate at which the lead was removed using batch kinetic studies. The results of the equilibrium studies were analyzed using the Langmuir and Freundlich isotherms. Although all of the equilibrium studies showed effective lead removal, neither the Langmuir nor the Freundlich isotherms properly quantified the data. In order to determine the influence of each of the independent variables, the percentage of lead removed was determined and plotted against either the alumina concentration or time the alumina was in solution. These plots displayed the percent of soluble lead removed versus alumina concentration or time for different pH values and presence of background matrices.

The results are organized by first showing the influence of pH on lead sorption. Next, the effects of background compounds on lead sorption is displayed where acetic acid and sodium chloride are the background matrices. Another perspective of the results is

presented by showing that lead sorption is an important removal technique at high pH ranges even though chemical precipitation plays a major role at these basic pH values. These results are shown for the equilibrium data first, followed by the time dependent kinetic data.

The results of the studies show that the greater the solution pH, the greater the amount and rate of soluble lead removal. The solution pH influences lead removal more than the other two variables that were examined in this study. The smaller alumina particles sorbed more lead at a faster rate than the larger particles. The influence of particle size is not as significant as the influence of pH. The presence of acetic acid influenced the amount and rate of lead removal, but not as much as pH. On the other hand, the presence of sodium chloride had little effect on the amount or rate of lead removal. From the results of the study, lead sorption using activated alumina is accomplished by the formation of a charged cloud of ions accumulating around the alumina particles and attracting oppositely charged ions. So in basic solutions, negatively charged OH^- ions predominate in the solution and accumulate around the alumina particles forming a negatively charged cloud. The negatively charged cloud attracts the positively charged lead ions, and the lead ions can be removed by filtering the alumina particles out of solution.

4.2 EQUILIBRIUM SORPTION DATA

4.2.1 Influence of pH on Lead Sorption

The influence of pH on soluble lead sorption is displayed by Figures 4.1 and 4.2. These plots show the percentage of lead removed versus the alumina concentration for four different pH values. The equilibrium sorption solutions were prepared with no background matrix. The results of Figures 4.1 and 4.2 show that more lead was removed at high pH than low pH. As the pH of the solution increases, the percentage of lead removed also increases. Another factor shown by these two plots is that sorption increases with decreasing alumina particle size. Figure 4.1 shows lead sorption for varying pH values using <74 μm alumina particles, while Figure 4.2 shows the same information using >1190 μm alumina particles. Comparing Figures 4.1 and 4.2, a larger percentage of lead was removed using the fine mesh particles at similar pH values. Figures 4.1 and 4.2 show the percentage of soluble lead removed. According to the pC-pH diagram for Pb-H_2O systems (see Figure 2.7), all of the soluble lead species at the given concentration of 40 mg/L and pH values no greater than 8.06 was Pb^{2+}. Some of the lead was removed through precipitation, but these figures only deal with the soluble species.

Figure 4.1 Influence of pH on Sorption of Lead with No Background Matrix and <74 Micron Mesh Alumina

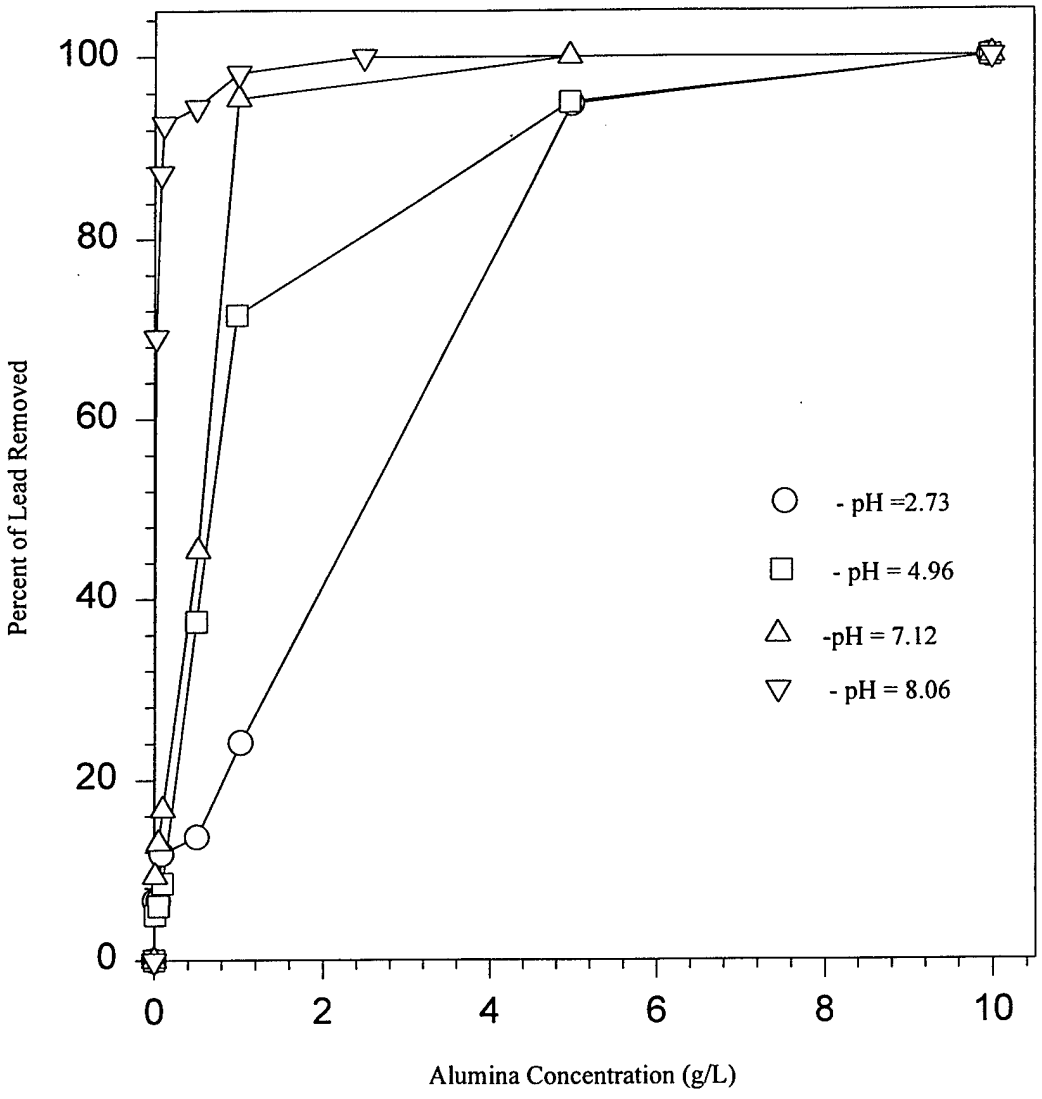

Figure 4.2 Influence of pH on Sorption of Lead with No Background Matrix and >1190 Micron Mesh Alumina

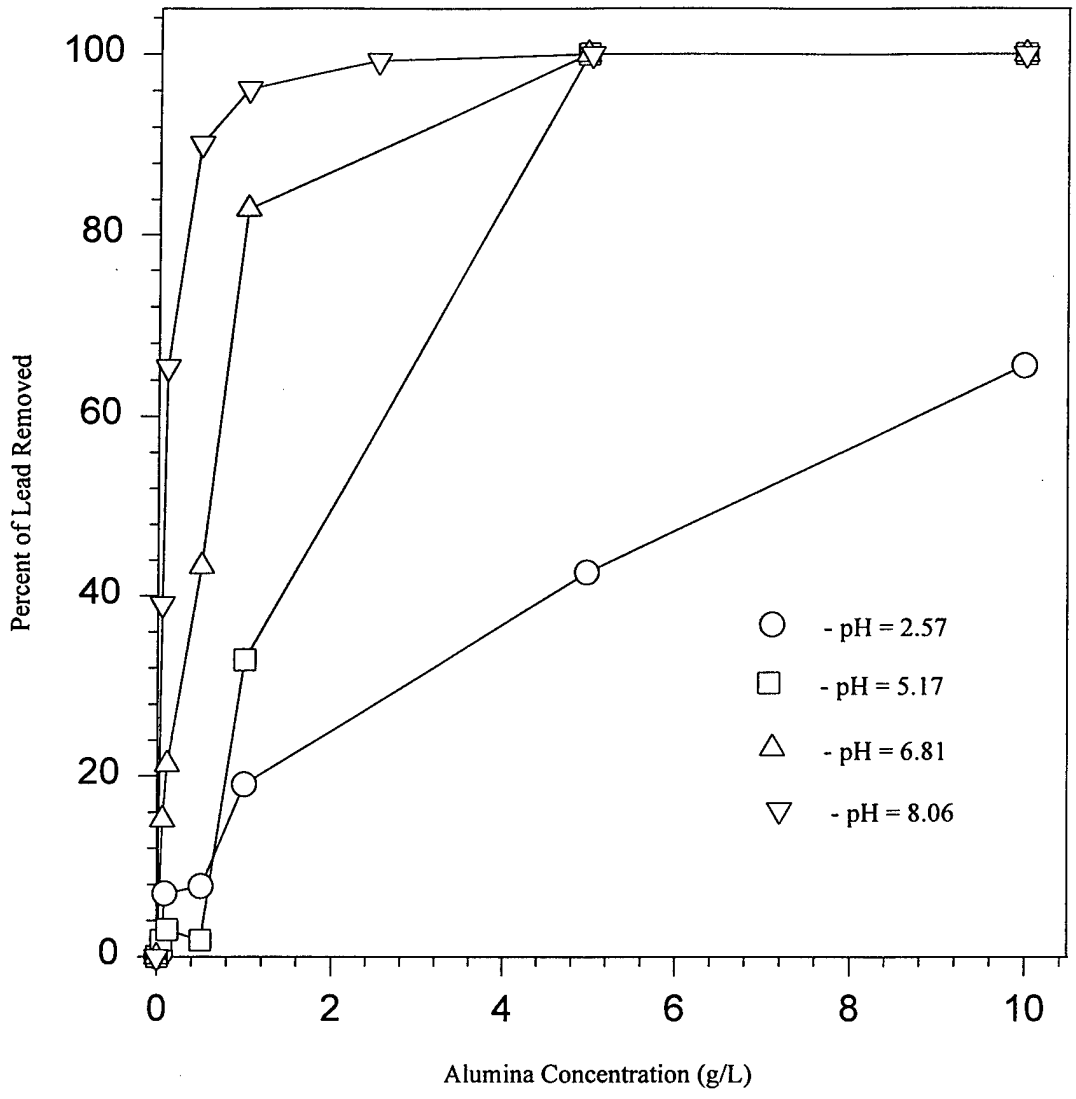

4.2.2 Influence of Background Matrices on Lead Sorption

4.2.2-A Acetic Acid Background Matrix

The influence of 1.0 mM acetic acid as a background matrix on soluble lead sorption is displayed by Figures 4.3 and 4.4. These figures show the percentage of lead removed versus alumina concentration at different pH values. Again as found in section 4.2.1, lead sorption is increased at higher pH and smaller alumina particle size. However, note that less lead was sorbed out of solution with the presence of acetic acid. The difference in the percentage of lead removed is apparent at high pH values, but it is much more significant at the low pH solutions. The presence of the competing acetic acid ions decrease soluble lead removal by increasing the positive electrical charge of the ion cloud around the alumina particles. This positive charge repels the positively charged lead ions.

Figures 4.3 and 4.4 show the amount of soluble lead removed. Therefore, precipitation is not taken into account when determining the percentage of lead removed. For the acidic pH values, no precipitation occurred and the lead species was Pb^{2+}. However, for the pH of 9.15, a small percentage (<10%) of the soluble lead species was $PbOH^{+}$.

4.2.2-B Sodium Chloride Background Matrix

The influence of sodium chloride as a background matrix on lead sorption is displayed by Figures 4.5 and 4.6. These figures show the percentage of lead removed versus alumina concentration at different pH values. Again, the solution at a pH value of 9.15 has a small percentage of $PbOH^+$ species in the solution. As in sections 4.2.1 and 4.2.2-A, lead sorption is higher for greater pH and smaller alumina particle size. However less lead was sorbed out of solution in the presence of sodium chloride. Figures 4.5 and 4.6 show that less lead was removed at high pH with the >1190 μm mesh particles. Interestingly, more lead was removed at the middle pH values with the sodium chloride matrix. Thus, a definitive conclusion cannot be drawn as to the influence of lead sorption in the presence of sodium chloride. It is shown in Figures 4.5 and 4.6 that a larger amount of lead is removed in the absence of acetic acid and sodium chloride background matrices, although the difference is small.

Figure 4.3 Influence of pH on Sorption of Lead with 1.0 mM Acetic Acid Background and <74 Micron Mesh Alumina

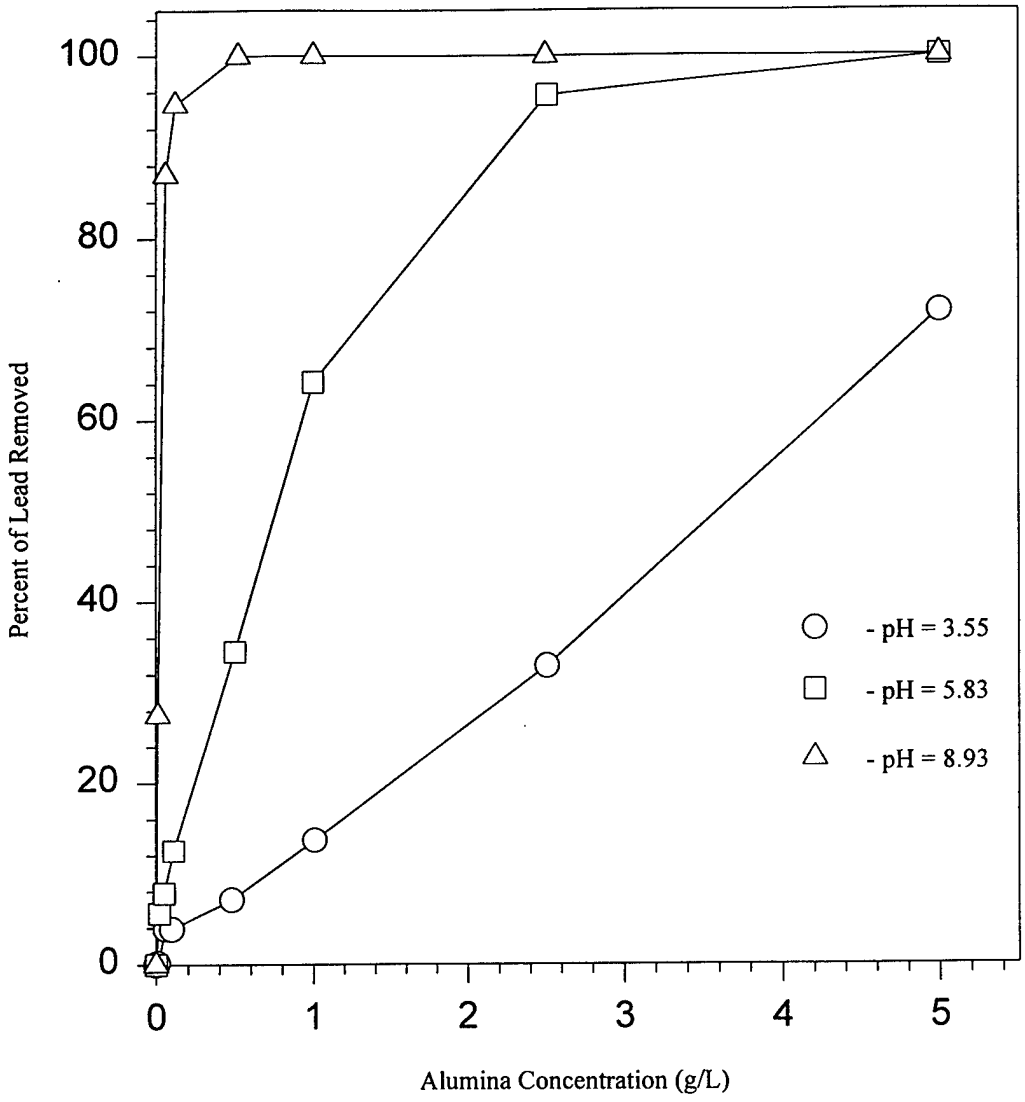

Figure 4.4 Influence of pH on Sorption of Lead with 1.0 mM Acetic Acid Background and >1190 Micron Mesh Alumina

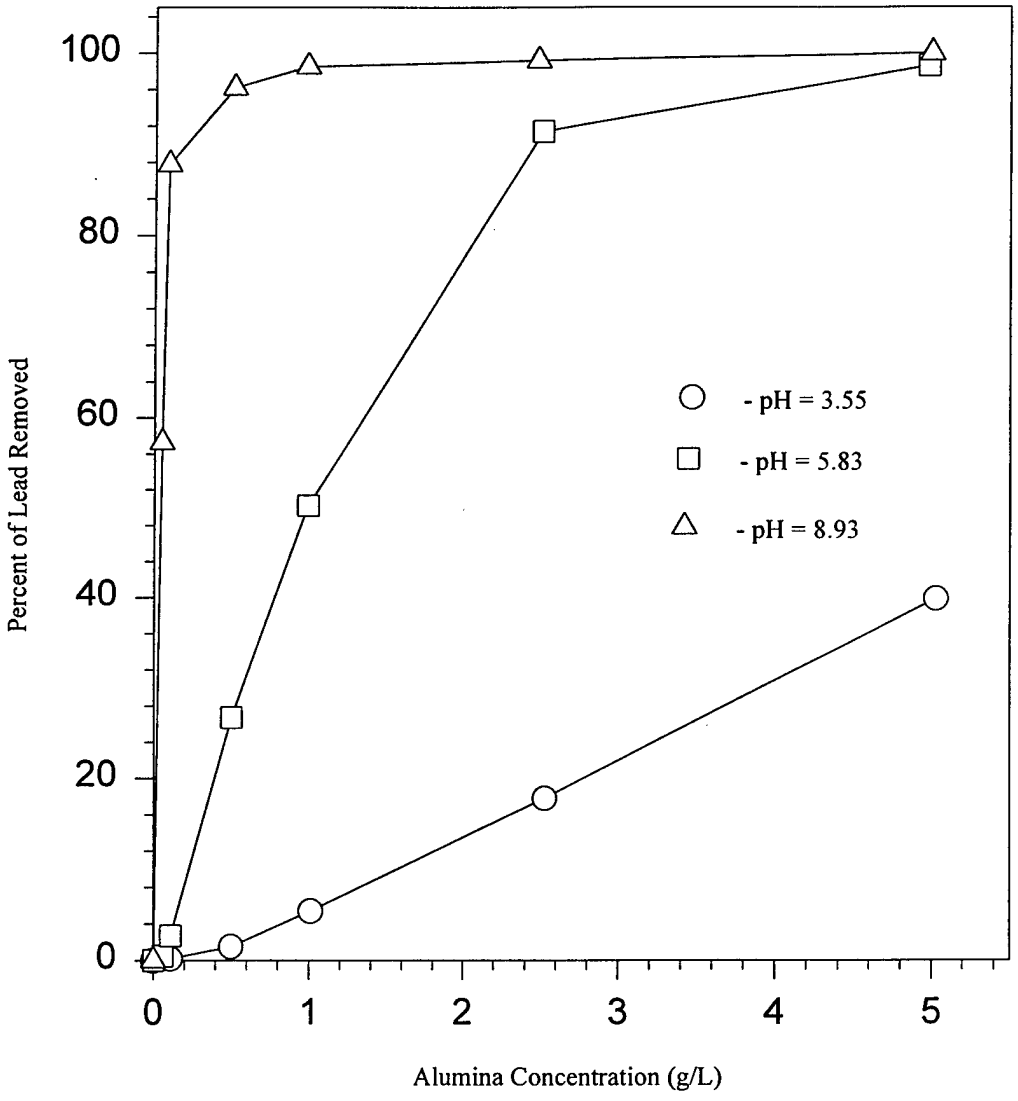

Figure 4.5 Influence of pH on Sorption of Lead with 0.1 mM Sodium Chloride Background and <74 Micron Mesh Alumina

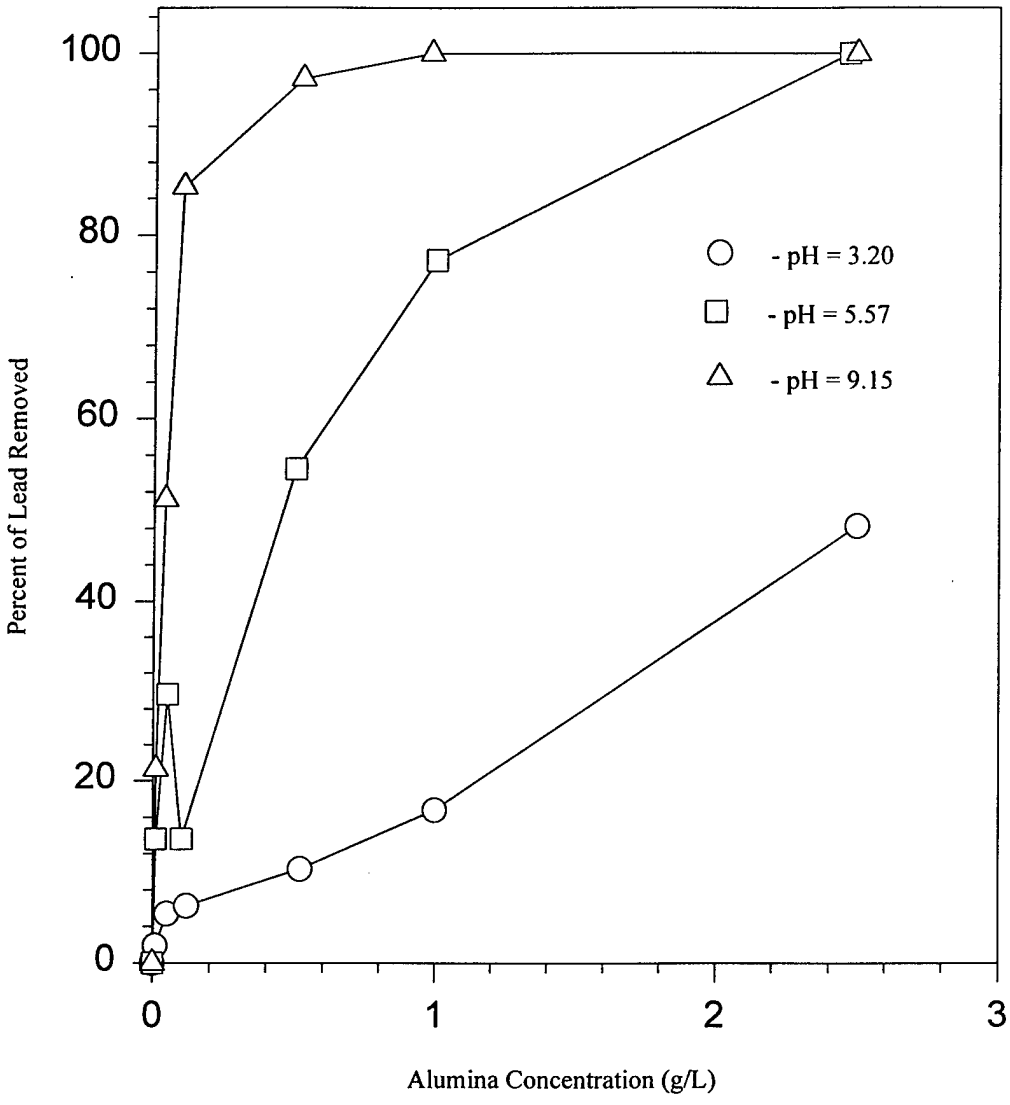

Figure 4.6 Influence of pH on Sorption of Lead with 0.1 mM Sodium Chloride Background and >1190 Micron Mesh Alumina

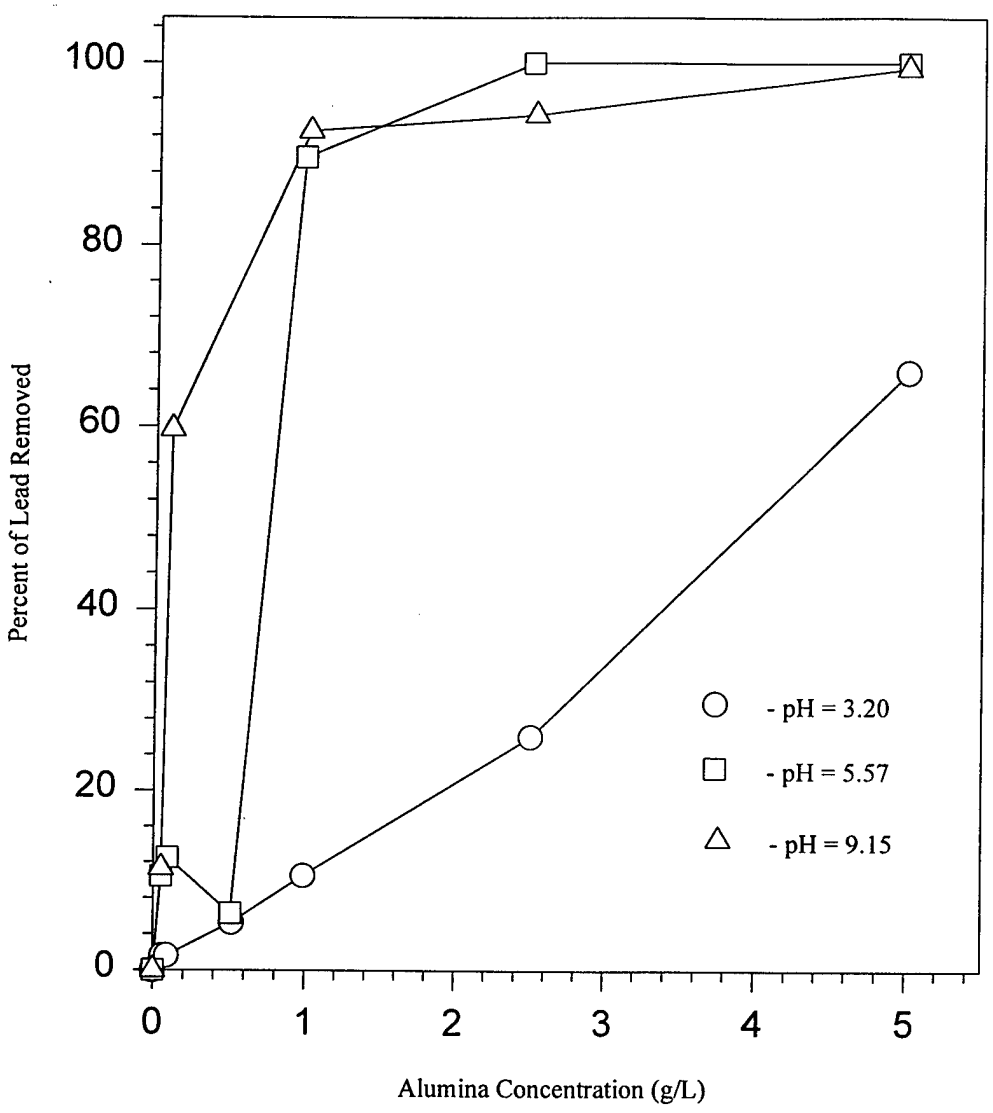

4.2.3 Influence of Elevated pH, Background Matrix Presence, and Particle Size

In comparing the influence of pH on lead sorption, it may seem that chemical precipitation is the only removal mechanism. This is not the case. Although the equilibrium sorption data were prepared with equal lead concentrations, the percentage of lead removed for the plots was calculated using the initial lead concentrations following precipitation. In all instances, the soluble lead sorbed onto the alumina particles (initial lead concentration in solution – final lead concentration in solution) was greater for the high pH solutions than low pH solutions. However, the soluble lead concentrations following precipitation were three to four times greater for the low pH solutions. Not only was there greater removal based upon the percentage of the initial lead concentration in high pH solutions, but more lead ions were sorbed, therefore removed from solution, in these basic solutions. Figures 4.7 and 4.8 show lead removal at high pH values for all of the variables. Note the difference in the percentage of lead removed in a sodium chloride matrix using the >1190 μm mesh alumina particles. When the alumina concentration was between 1 – 3g/L, the percentage of lead removed in the sodium chloride matrix was between 5-10% less than that for the solution without the presence of a background matrix. This difference in the percentage of lead removed cannot be due to chemical precipitation, but to the sorption of lead onto the alumina particles.

Figure 4.7 Influence of Background Matrix on Sorption of Lead with <74 Micron Mesh Alumina

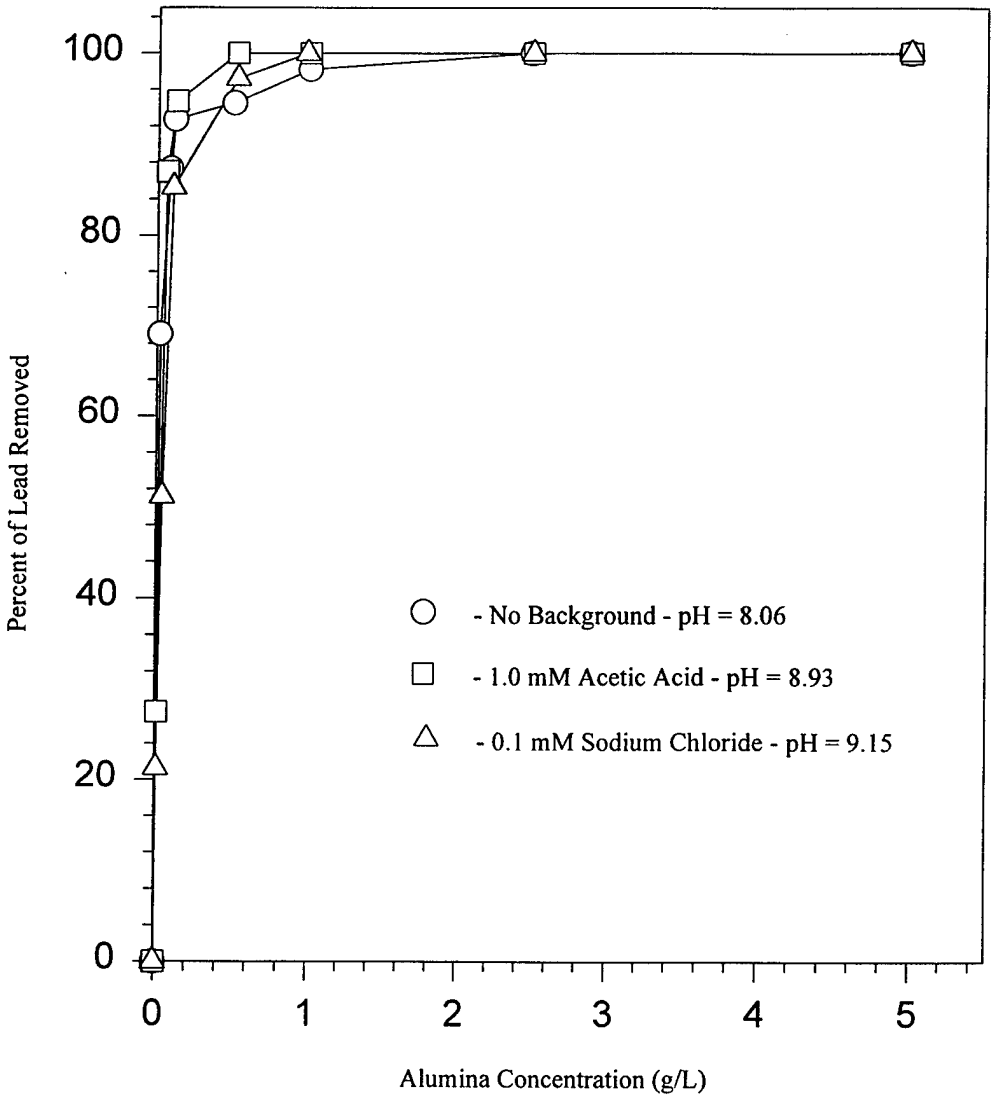

Figure 4.8 Influence of Background Matrix on Sorption of Lead with >1190 Micron Mesh Alumina

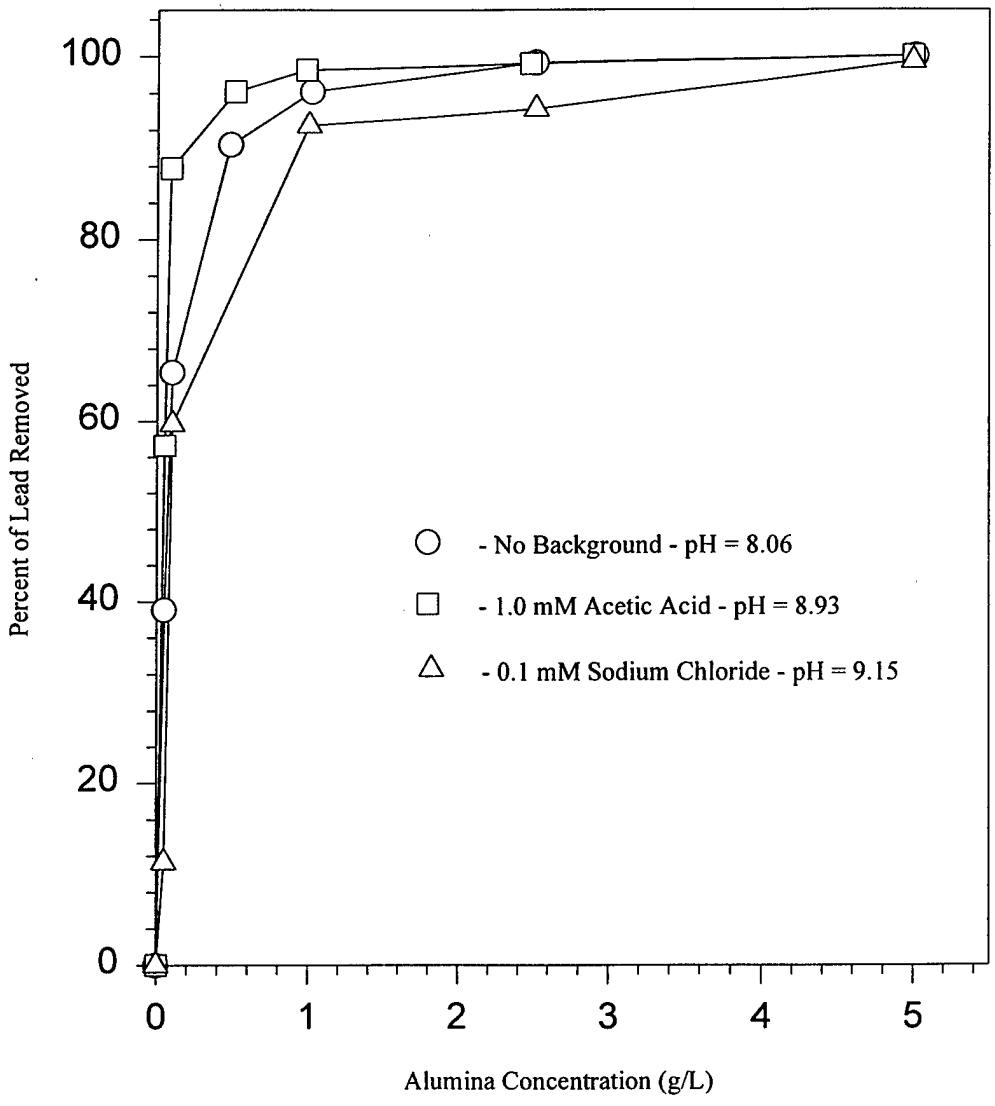

4.3 KINETIC SORPTION DATA

4.3.1 Influence of pH on Rate of Lead Sorption

The influence of pH on rate of lead sorption is displayed by Figures 4.9 and 4.10. These plots show the percentage of soluble lead removed versus the time the alumina was in solution. All of the kinetic tests were run with an alumina concentration of 1.0 g/L and a lead concentration of 20mg/L or 40 mg/L. The tests were conducted without the presence of a background matrix. The data of Figures 4.9 – 4.16 show similar results as the equilibrium studies. As the pH of the solution increased, the percentage of lead removed from solution also increased. Further, the rate of lead removed was much faster for the high pH solutions. The soluble lead species present in the solutions with pH values less than 8.0 was Pb^{2+}, but the solutions with pH values greater than 8.0 contained a small percentage of $PbOH^{+}$ and $Pb(OH_3)^{-}$ species. By inspecting the two plots, the <74 μm mesh alumina particles removed much more lead than the >1190 μm mesh particles. The small diameter particles also removed lead at a much faster rate than the larger diameter particles.

Figure 4.9 Influence of pH on Rate of Lead Sorption with No Background Matrix and <74 Micron Mesh Alumina

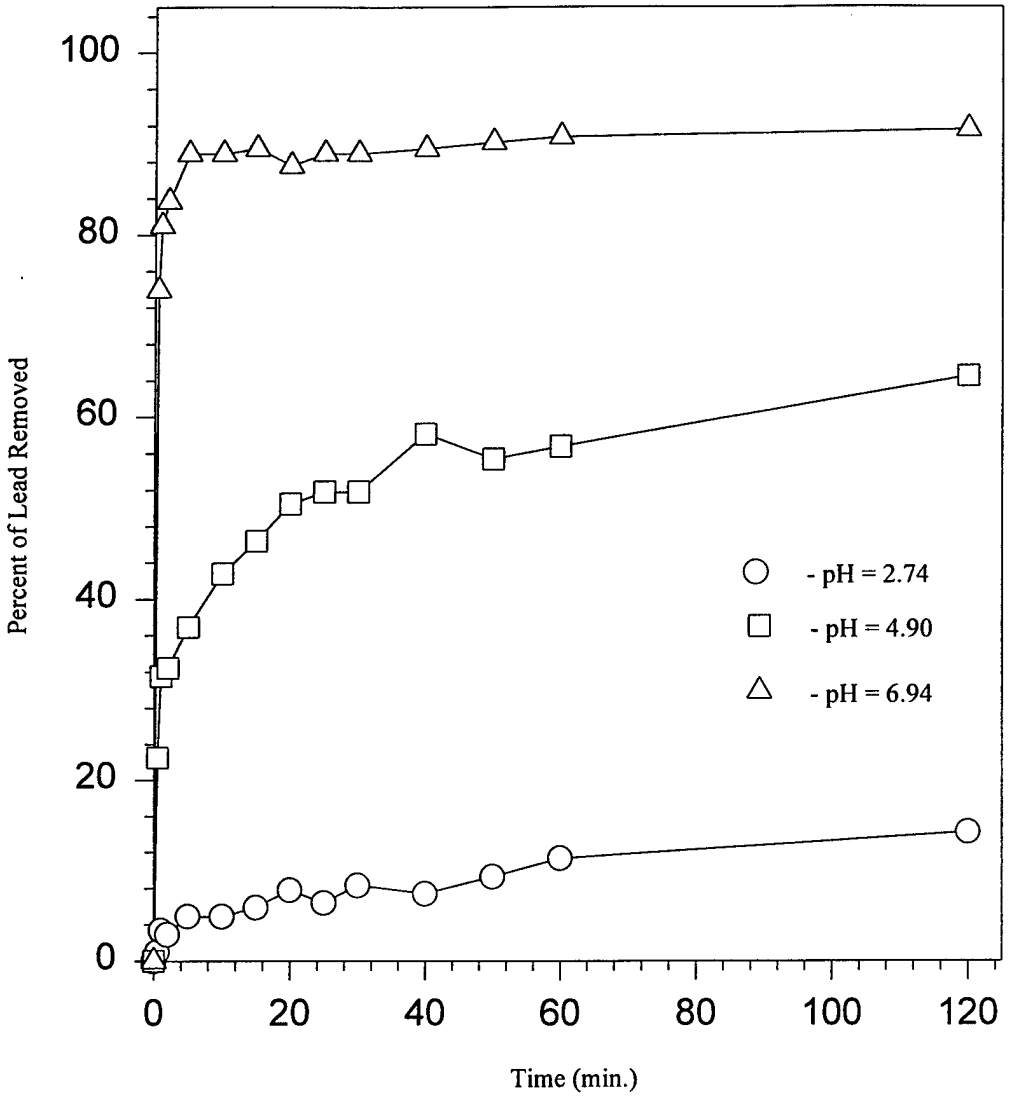

Figure 4.10 Influence of pH on Rate of Lead Sorption with No Background Matrix and >1190 Micron Mesh Alumina

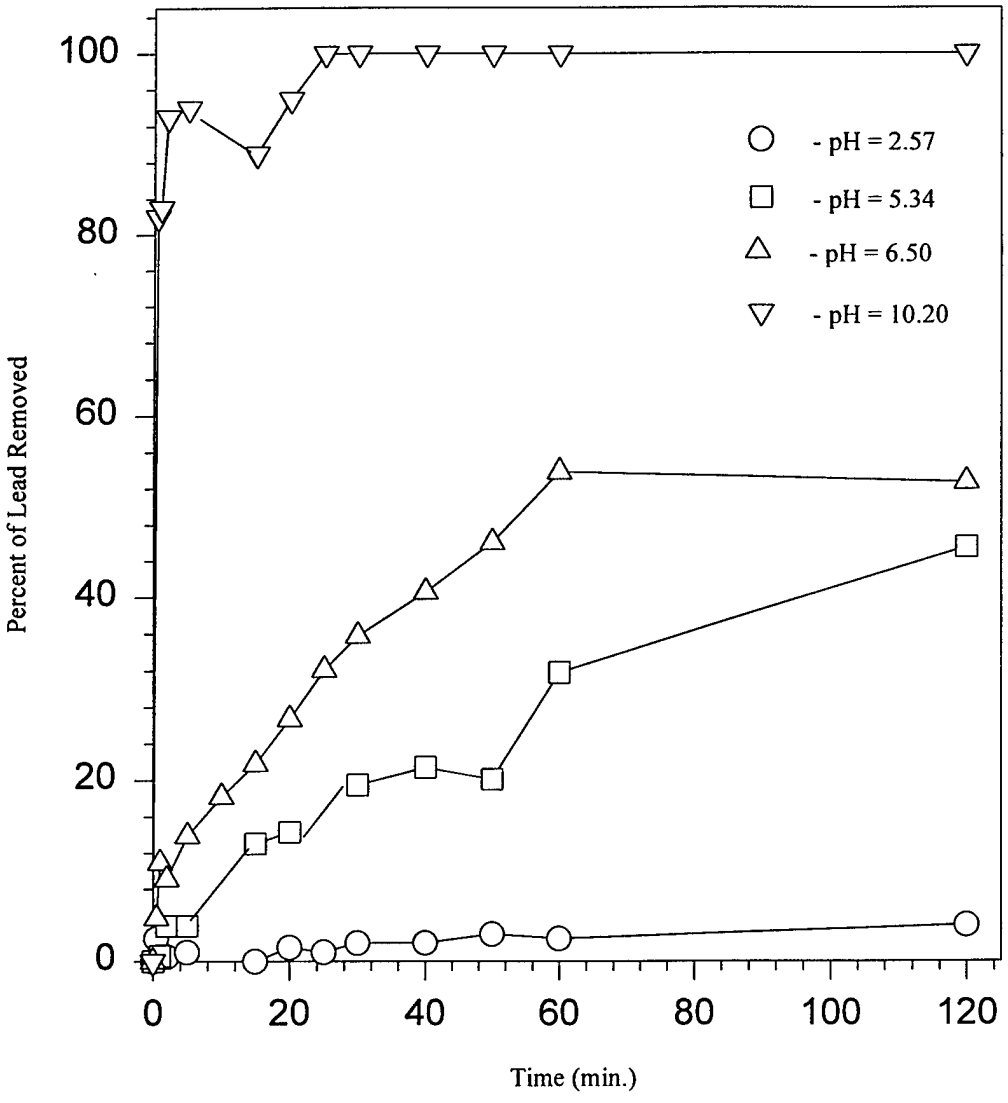

4.3.2 Influence of the Presence of Background Matrices on Rate of Lead Sorption

4.3.2-A Acetic Acid Background Matrix

The presence of 1.0 mM acetic acid as a background matrix on rate of lead sorption is displayed in Figures 4.11 and 4.12. These figures show the percentage of soluble lead removed versus the time the alumina was in solution. Plots in Figures 4.11 and 4.12 show that lead was removed from solution at a much faster rate for the solutions at higher pH values. Also, the <74 μm mesh alumina particles removed lead at a greater rate than the >1190 μm mesh particle size. Figures 4.11 and 4.12 also show that less lead was sorbed, and at a much slower rate in the presence of the acetic acid background matrices as opposed to the kinetic plots for the lead solutions with no background matrix at comparable solution pH. This reduction in lead sorption can be attributed to the presence of competing ions which give a positive charge to the cloud surrounding the alumina particles.

4.3.2-B Sodium Chloride Background Matrix

The influence of 0.1 mM sodium chloride added as a background matrix on the rate of soluble lead sorption is displayed by Figures 4.13 and 4.14. These figures show the percentage of soluble lead removed versus the time the alumina was in solution at different pH levels. Again, more lead was removed from solution at higher pH values. Differences in the lead removal rate as a function of particle size is not as conclusive for

these data (Figures 4.13 and 4.14) as was found in the equilibrium studies. The rate of lead sorption in solutions containing the sodium chloride matrix does not differ much from the solutions containing no background matrix as shown by comparing Figures 4.9, 4.10, 4.11, and 4.12. The rate and amount of sorption was much greater for the solutions containing no background matrix and/or sodium chloride matrix than the solutions containing the acetic acid background matrix.

Figure 4.11 Influence of pH on Rate of Lead Sorption with 1.0 mM Acetic Acid Background and <74 Micron Mesh Alumina

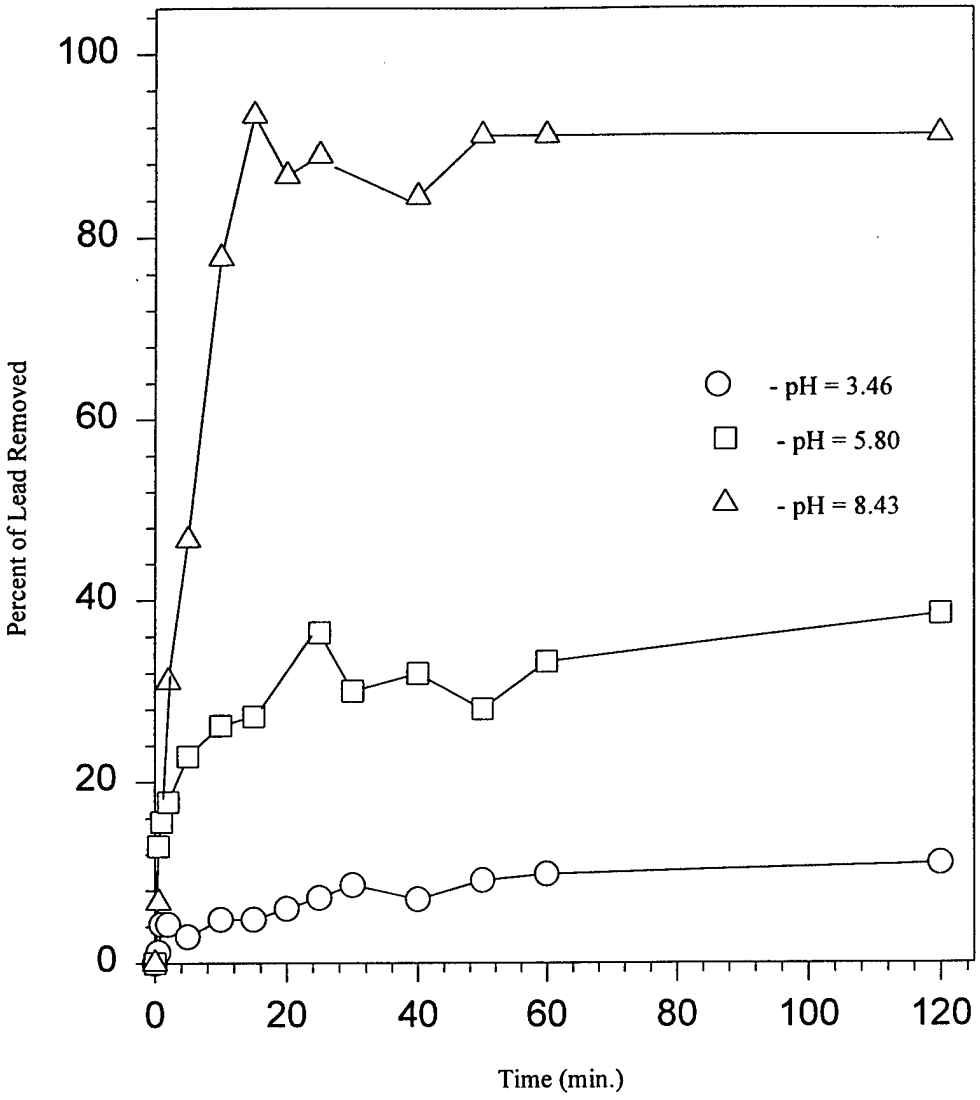

Figure 4.12 Influence of pH on Rate of Lead Sorption with 1.0 mM Acetic Acid Background and >1190 Micron Mesh Alumina

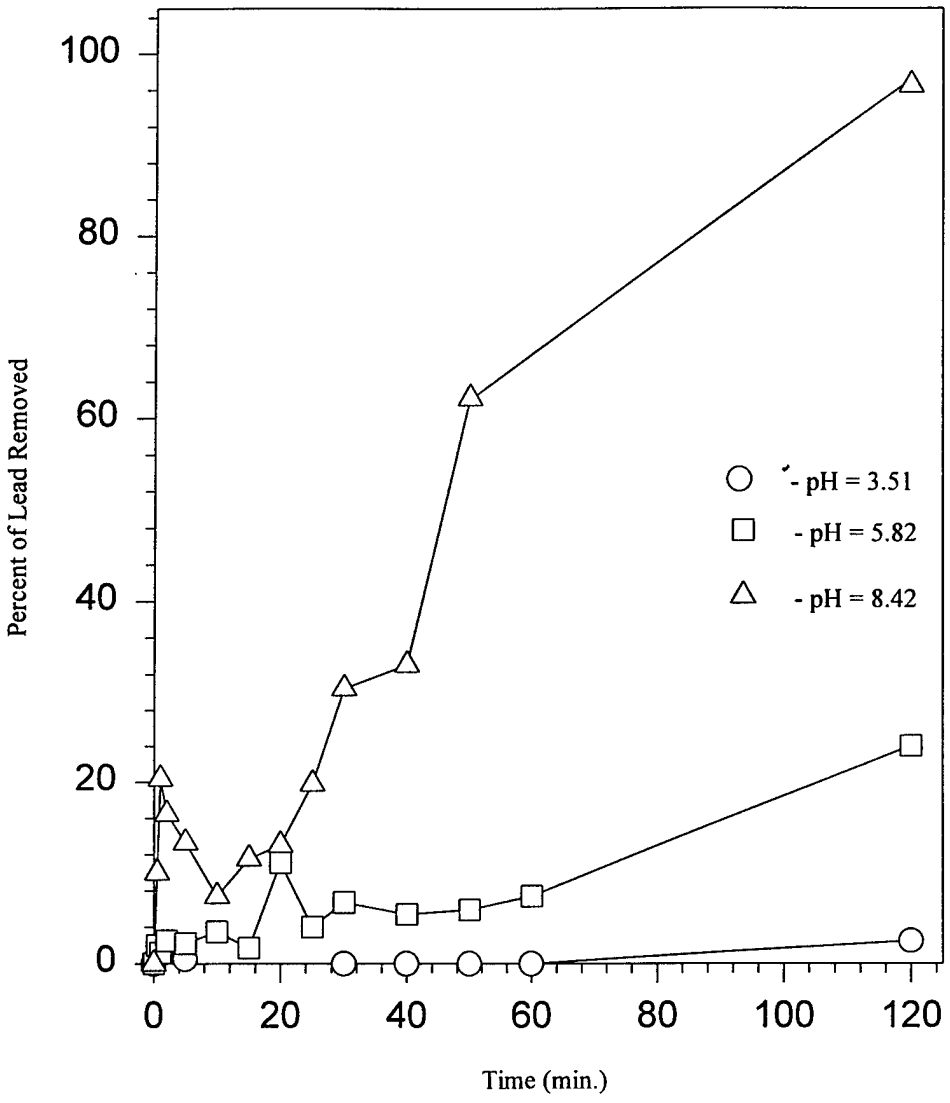

Figure 4.13 Influence of pH on Rate of Lead Sorption with 0.1 mM Sodium Chloride Background and <74 Micron Mesh Alumina

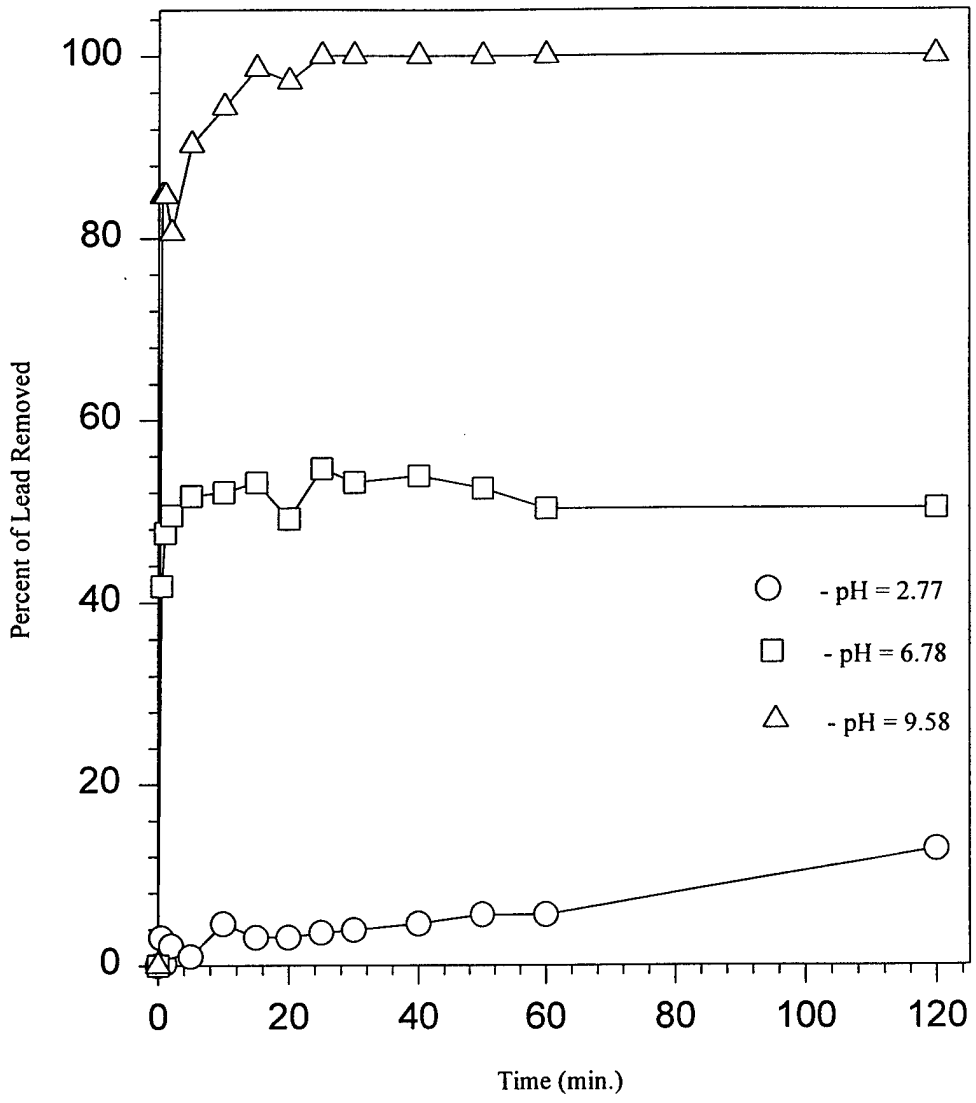

Figure 4.14 Influence of pH on Rate of Lead Sorption with 0.1 mM Sodium Chloride Background and >1190 Micron Mesh Alumina

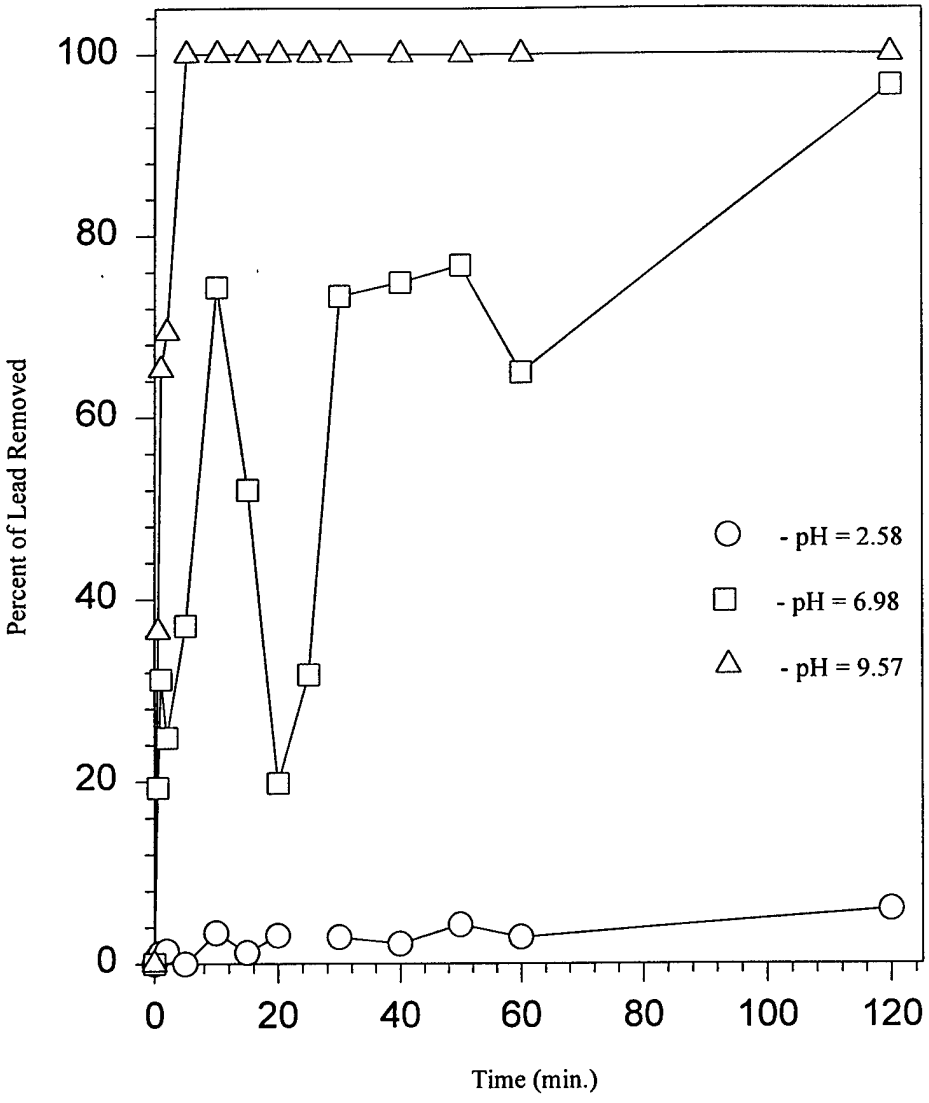

4.3.3 Influence of Elevated pH, Background Matrix, and Particle Size on Rate of Lead Sorption

Figures 4.15 and 4.16 show several patterns in the use of alumina in removing soluble lead from aqueous solutions. Figure 15 shows lead sorption rate occurring at nearly neutral pH values. The solution without a competing background matrix removes lead much faster than the other two solutions containing additional complexes. This can be attributed to the presence of additional ions giving a positive charge in the cloud surrounding the alumina particles. In Figure 4.16, the sorption of lead with the varying background matrices is shown for high pH values. The sorption of lead in solutions containing acetate ion at a pH of 8.42 shows a very slow rate of sorption compared to the other two solutions. The plot of the acetic acid background also shows that chemical precipitation is not the only mechanism involved in lead removal since a large portion of the lead remained in solution despite the high pH. Also, the solution without the presence of a competing background matrix shows higher rates of sorption than the solutions containing the sodium chloride matrix, although the difference in the rates is not very significant. Figures 4.15 and 4.16 show that lead is more readily sorbed onto alumina particles in higher pH solutions.

Figure 4.15 Influence of Background Matrix on Rate of Lead Sorption with <74 Micron Mesh Alumina

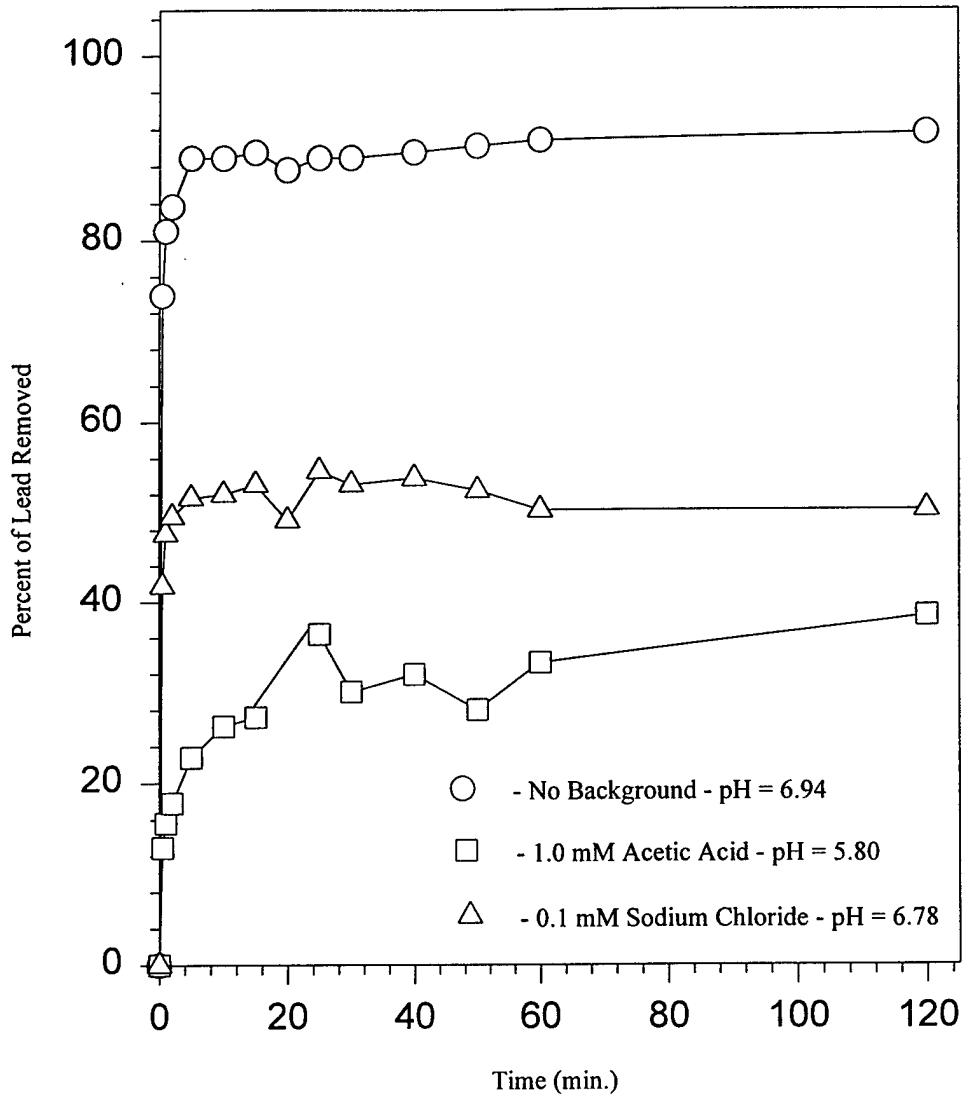

Figure 4.16 Influence of Background Matrix on Rate of Lead Sorption with >1190 Micron Mesh Alumina

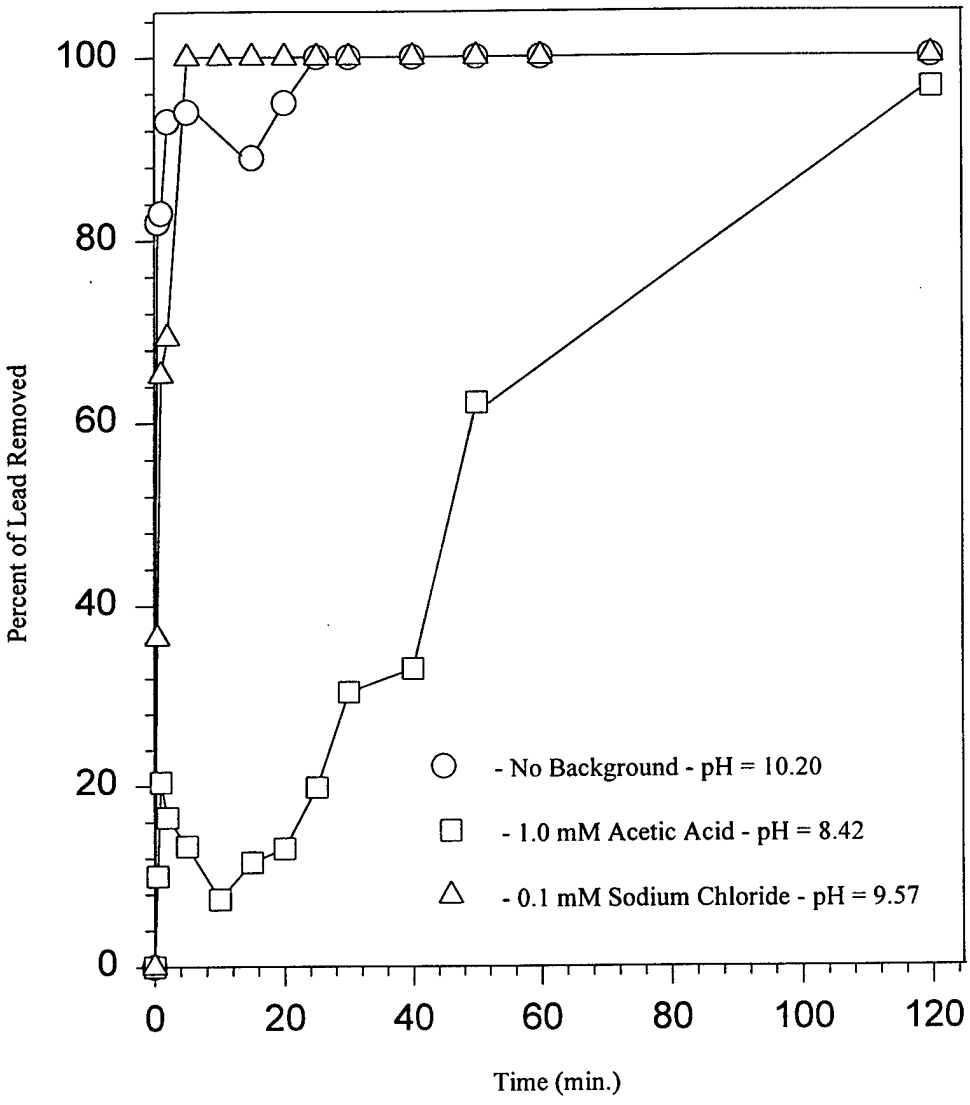

5. CONCLUSIONS

Results of the investigation successfully demonstrate the ability of aluminum oxide (γ-Al_2O_3) to effectively remove lead from aqueous solutions. Effectiveness of lead removal using alumina was shown to be dependent upon several variables. As evaluated in this research, solution pH, alumina particle size, and competing ions associated with background matrices influence the amount and rate of lead removal using activated alumina.

Solution pH plays a key role in the effectiveness of lead sorption using alumina. The higher the pH, the greater the percentage of soluble lead removed. In addition, the rate of soluble lead sorption is much faster for high pH solutions. At high pH values, chemical precipitation may also play a significant role in lead removal. The results of this study show the percentage of lead removed after chemical precipitation has occurred. The results shown in figures 4.1 – 4.16 indicate the percentage of soluble lead removed due to alumina sorption only. Since a large amount of lead is precipitated in basic solutions, the initial lead concentration in acidic solutions is larger than basic solutions. This may lead to some skew in the numbers, but the data shows a larger concentration of lead removed in basic solutions. The reason for the higher percentage of lead removal in basic solutions is due to the fact that at lower pH values there are more hydrogen ions in

solution. These hydrogen ions collect around the alumina particles giving the alumina-hydrogen ion cloud a positive charge. This positive charge repels the positively-charged lead ions in solution. On the other hand, at high pH values, negatively charged OH^- ions predominate and form a cloud around the alumina particles creating a negative charge. This negative charge attracts the positively charged lead ions to collect around the aluminum-hydroxide cloud (see Figure 5.1).

Alumina particle size was also found to influence both the rate and equilibrium amount of lead sorption. The smaller the alumina particle size, the larger the amount of lead removed. Further, the smaller particle size alumina demonstrated faster rate of lead sorption. The reason for the influence of particle size is due to the fact that the smaller particle size has larger surface area per gram of alumina added to the solutions. The increased surface area leads to an increase in the area around which the charged ions may accumulate around the alumina particles. The influence of particle size is noticeable in the data, but it is not as significant as the influence of pH solution.

Competing ions associated with acetic acid and sodium chloride background influence the rate and amount of lead sorption. The presence of competing ions decreases the rate and amount of lead sorbed. Equilibrium lead sorption capacity and the rate of lead sorption using alumina was greater for solutions which did not contain background matrices. The presence of acetate ion represents the influence of organic compounds, while sodium chloride represents the influence of inorganic compounds. The data shows that sorption occurred faster in sodium chloride matrices than acetic acid solutions. The

Figure 5.1: Diagram of Ion Cloud Formation Around Alumina Particle (from Clark, 1996)

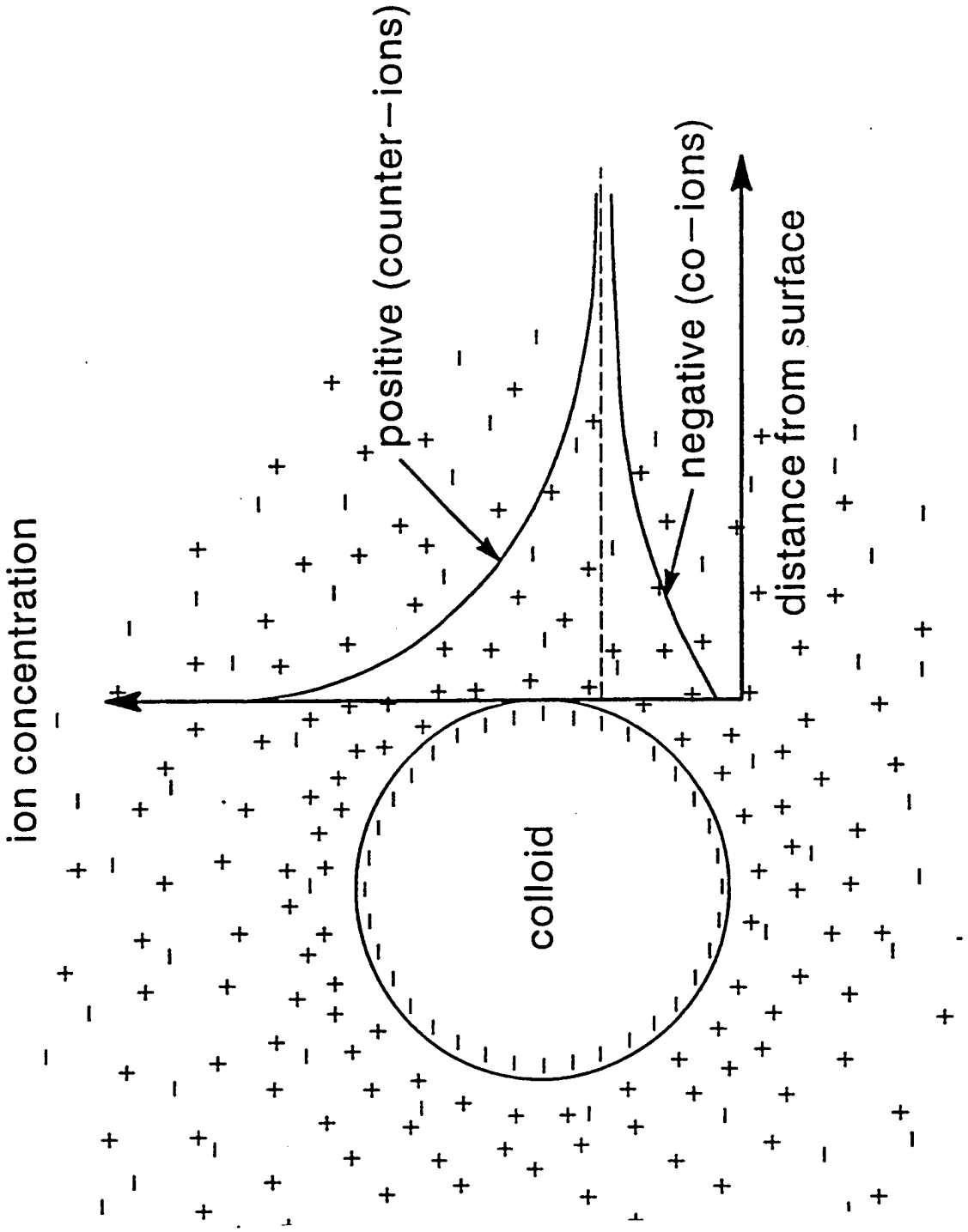

reason that sorption is faster and equilibrium capacity greater in the solutions without background matrices is that there are no "extra" ions adding an additional positive charge in the cloud surrounding the alumina particle.

The results of this research show that the removal of lead from aqueous solutions using activated alumina cannot be described as simple adsorption. The data obtained from the equilibrium and kinetic studies reveal that the lead cations do not permanently attach to the aluminum particles. If the lead cations leave solution and permanently attach to the alumina particles, then the solution pH should increase due to the removal of the positively charged lead ions. The pH of the solution did not change when alumina was added to either the equilibrium or kinetic studies. Also, the equilibrium data was plotted to Freundlich and Langmuir adsorption isotherm equations, and neither of the isotherm equations could properly describe lead removal. This leads to the assumption that another type of removal model should be used to describe the sorption of lead using activated alumina.

Ion exchange is another type of removal mechanism that is used to describe metal removal. Again, ion exchange is a permanent reaction where the lead cations stay attached to the alumina particles. The absence of a pH change with the addition of alumina leads to the belief that ion exchange is not the removal mechanism responsible for lead sorption.

The lack of a significant pH change points out that the hydrogen and lead ions do not permanently dissociate, but form a cloud around the alumina particles. The lead cations

are not tightly bound to the alumina particles, but they are associated to the particles by pH and ionic strength.

The data shows that the lead sorption in this study is most likely due to the prevalence of the lead cations to gather in the diffuse double layer around the alumina particles. The Debye-Huckel model for the double layer has a surface cloud of counter ions around the alumina particle. The Debye-Huckel model assumes that there is only a small electrical potential, and that the electrical charges will not be large. The thickness of the double layer ($1/\kappa$) is can be determined using equation 5.1 (Clark, 1996).

$$\kappa^2 = \frac{e^2 \sum_i z_i^2 n_{i0}}{\varepsilon \varepsilon_0 kT} \qquad \textbf{(5.1)}$$

where;

κ = inverse length of double layer

e = proton charge (1.60219×10^{-19} C)

z_i = valence of the ith-type ion

n_{io} = number of the ith-type ions per cubic centimeter at an infinite distance from the surface

ε = relative permittivity of the medium

ε_0 = permittivity in a vacuum (8.854×10^{-14} C^2 cm^{-1} J^{-1})

k = Boltzmann constant (1.38066×10^{-23} JK^{-1})

T = temperature .

Finally, the valence of the species removed by alumina influences the amount of metal sorption using the double layer model. Equation 5.1 shows that the higher the valence, the smaller the double layer thickness. This valence dependence would point to metal sorption increasing as the valence of the metal ion increases. In research conducted by Wootton *et al.* (1998), several metal species were removed from aqueous solutions using activated alumina. The studies of Wootton *et al.* found that sorption increased with increasing metal valence. Monovalent metals (1^+) showed little or no sorption, while in the polyvalent metals the rate and amount of sorption increased as the valence increased. Selenium (5^+) cations showed the greatest metal sorption in the study of Wootton *et al.* Also, in studies conducted by Reed (1998) dealing with the sorption of anions using activated alumina, anion sorption increases as the solution pH decreases. This study supports the theory that sorption using activated alumina is due to the formation of a charged cloud surrounding the alumina particles. As solution pH increases, the cloud around the alumina particle should be positively charged, and attract the negatively charged anions.

Results of this study and the previous studies of Wootton *et al.* indicate that lead removal using activated aluminum oxide is a viable treatment mechanism. It appears from these data that lead sorption is a surface complexation phenomenon best described using the diffuse layer model. Lead sorption occurs more rapidly and abundantly in basic solutions with fine mesh alumina particles in solutions that contain few competing ions. Given the improvement in lead sorption at increased pH levels, it seems prudent to

suggest that lead sorption using activated alumina could be improved by prewashing the alumina particles in a basic solution.

6. REFERENCES

Adamson. (1990). Physical chemistry of surfaces. 5th edition. John Wiley & Sons, Inc.776.

Ahmed, S., S. Chugtai, M.A. Keane. (1998). The removal of cadmium and lead from aqueous solution by ion exchange with Na-Y zeolite. *Separation and Purification Technology*. 13, 57-64.

APHA (American Public Health Association) (1992). *Standard Methods for the Examination of Water and Wastewater (18th ed.)*., American Public Health Association. Washington, D.C.

Baes, C.F., R.E. Mesmer. (1976). The hydrolysis of cations. Krieger Publishing Company. 358-365.

Barrow, N.J. (1978). Effect of previous additions of phosphate on phosphate adsorption by soils. *Soil Sci.* 118:902-907.

Barrow, N.J. (1986). Testing a mechanistic model. II. The effects of time and temperature on the reaction of zinc with a soil. *J. Soil Sci.* 37:277-286.Barrow, N.J. (1989). Testing a mechanistic model. X. The effects of pH and electrolyte concentration on borate sorption by a soil. *J. Soil Sci.* 40:427-435.

Barrow, N.J., J. Garth, and G.W. Brummer. (1989). Reaction kinetics of the adsorption and desorption of nickel, zinc, and cadmium by geothite. II. Modeling the extent and rate of reaction. *J. Soil Sci.* 40: 437-450.

Barrow, N.J., J.W. Bowden, A.M. Posner, and J.P. Quick. (1980). An objective method for fitting models of ion adsorption on variable surface charge. *Aust. J. Soil Res.* 18:37-47.

Barrow, N.J., J.W. Bowden, A.M. Posner, and J.P. Quick. (1981). Describing the adsorption of copper, zinc, and lead on a variable charge mineral surface. *Aust. J. Soil. Res.* 19: 309-321.

Bowden, J.W., A.M. Posner, and J.P. Quick. (1977). Ionic adsorption on variable charge mineral surface. Theoretical-charge development and titration curves. *Aust. J. Soil Res.* 15: 121-136.

Bowden, J.W., S. Nagarajah, N.J. Barrow, A.M. Posner, and J.P. Quick. (1980). Describing the adsorption of phosphate, citrate, and selenite on a variable charge mineral surface. *Aust. J. Soil Res.* 18: 49-60.

Brower, J.B., R.L. Ryan, and M. Pazirandeh. (1997). Comparison of ion-exchange resins and biosorbents for the removal of heavy Metals from plating factory wates. *Environ. Sci. Technol.* 31: 2910-2914.

Buchter, B., B. Davidoff, M.C. Amacher, C. Hinz, I.K. Iskander, and H.M. Selim. (1989).Correlation of Freundlich K_d and n retention parameters with soils and elements. *Soil Sci.* 148: 370-379.

Carell, B. and A. Olin. (1962). Studies on hydrolysis of metal ions. A thermochemical study of hydrolysed Pb solutions. *Acta. Chem. Scand.* 16:4.

Clark, M.M. (1996). Transport Modeling for Environmental Engineers and Scientists.John Wiley & Sons. 71-142.

Davis, J.A. and D.B. Kent. (1990). Surface complexation modeling in aqueous geochemistry. P. 177-260. In M. F. Hochella and A.F. White (ed.) Mineral-water Interface Geochemistry. Reviews in Minearology, V. 23. MSA, Washington, D.C.

Davis, J.A., R.O. James, and J.O. Luckie. (1978). Surface ionization and complexation at the oxide/water interface. I. Computation of electrical double layer properties in simple electrolyte. *J. Colloid Interface Sci.* 63: 480-499.

Dzomback, D.M. and M.M. Morel (1986). Sorption of cadmium on hydrous ferric oxide at high sorbate/sorbent ratios. *J. Colloid Interface Sci.* 112: 588-598.

Dzomback, D.M. and M.M. Morel (1990). Surface complexation modeling. John Wiley & Sons, New York. 385.

Edwards, J.D., K.W. Bayha, A.J. Abbott, and J.W. Ryznar. (1947). Aluminum compounds – alumina and the hydrated aluminas. *Kirk-Othmer Encyclopedia of Chemical Technology*. John Wiley. Volume 1. 1st Edition. 640-653.

Esval, O. and J.S. Johnson, Jr. (1965). Equilibrium ultracentrifugaton of hydroloyzed lead (II) perchlorate solutions. *J. Phys. Chem.* 69: 959.

Fox, R.L. and E.J. Kamprath. (1970). Phosphate sorption isotherms for evaluating the phosphate requirements of soils. *Soil Sci. Am. Proc.* 34: 902-907.

Freidline, C.E. and R.S. Tobias. (1966). Raman spectroscopioc and EMF studies on aqueous solutions of trans-tetrahydroxidodimethyls tannate (IV) ion. *Inorganic Chemistry*. 5: 34.

Goldberg, S. (1992). Use of surface complexation models in soil chemical systems. *Adv. Agr.* 47: 233-329.

Goodboy, K.P.and H.L. Fleming. (1984). Trends in adsorption with aluminas. *Chemical Engineering Progress.* 63-68.

Harding, I.H. and T.W. Healy. (1985a.). Adsorption of aqueous cadmium(II) on amphoteric latex colloids. *J. Colloid Interface Sci.* 107: 371-381.

Harding, I.H. and T.W. Healy. (1985b.). Electrical double layer properties of amphoteric polymer latex colloids. *J. Colloid Interface Sci.* 107-382-397.

Hayes, K.F. (1987). Equilibrium, spectroscopic and kinetic studies of ion adsorption at the oxide/aqueous interface. Ph.D. Dissertation, Stanford University, Stanford, California. 260.

He, L. (1995). Adsorption of sulfate and Phosphate at the mineral-water interface: isotherm, stoichiometry, and minerals. Ph.D. Dissertation, Virginia Polytechnic Institute and State University, Blacksburg, Virginia. 10-45.

Hohl, H and W. Stumm. (1976). Interaction of Pb^{2+} with hydrous γ-Al_2O_3. *J. Colloid Interface Sci.* 55: 281-288.

Holm, T.R. and X.F. Zhu. (1994). Sorption by kaolinite of Cd^{2+}, Pb^{2+}, and Cu^{2+} from landfill leachate-contaminated groundwater. *Journal of Contaminant Hydrology.* 16: 271-287.

Johansso, G. and A. Olin. (1968). On structures of dominating hydrolysis products of lead (II) in solution. *Acta. Chem. Scand.* 22: 3197.

Lee, D.R. , J.M. Hargreaves, L. Badertscher, and F. Kassir. (1995). Reverse osmosis and activated alumina water treatment plant for the California state prisons located near Blythe. *Desalination.* 103: 155-161.

Lovgren, L., S. Sjoberg, and P.W. Schindler. (1990). Acid/base reactions and Al(III0 complexation at the surface of geothite. *Cosmochim. Acta.* 54: 1301-1306.

Maroni, V.A. and T.G. Spiro. (1967). Vibrational spectrum of polynuclear hydroxy complexes of lead (II). *Journal of American Chemical Society.* 89:45.

Mehadi, A.A. and R.W. Taylor. (1988). Phosphate adsorption by two highly weathered soils. *Soil Sci. Soc. Am. J.* 52: 627-632.

National Bureau of Standards. (1968). Selected values of chemical thermodynamic properties. Technical notes. U.S. Govt. Printing. Off., Washington, D.C. 270-274.

Orumwense, F.F. (1996). Removal of lead from water by adsorption on a kaolinitic clay. *J. Chem. Tech. Biotechnol.* 65: 363-369.

Osaki, S., T. Miyashi, S. Sugihara, and Y. Takashima. (1990a.). Effects of metal ions and organic ligands on the adsorption of Co (II) onto silica gel. *Sci. Total Environ.* 99: 93-103.

Osaki, S., T. Miyashi, S. Sugihara, and Y. Takashima. (1990b.). Adsorption of Fe(II), Co(II), and Zn(II) onto particulates in fresh waters on the basis of the surface complexation model. I. Stabilities of metal species adsorbed on particulates. *Sci. Total Environ.* 99: 105-114.

Papee, D. and R. Tertian. (1963). Aluminum compounds – Aluminum oxide (Alumina). *Kirk-Othmer Encyclopedia of Chemical Technology.* John Wiley. Volume 2. 2nd edition. 41-58.

Pearson, A., G. MacZura, and C. Misra. (1992). Aluminum compounds (activated). *Kirk-Othmer Encyclopedia of Chemical Technology.* John Wiley. Volume 2. 4th edition. 291-330.

Pleissner, M. (1907). *Arb. Kaiserl. Gesundheitsamte.* 26. 384.

Posner, A.M. and J.W. Bowden. (1980). Adsorption isotherms: should they be split?. *J. Soil Sci.* 31:1-10.

Ram, W., R.N. Prasad, and P. Ram. (1987). Studies on phosphate adsorption and phosphate fixation in Alfisols and Entisols occurring in different altitudes of Meghalaya. *J. Indian Soc. Sci.* 35: 207-216.

Reed, B.E. and S. Arunachalam. (1994). Use of granular activated carbon columns for lead removal. *J. Environ. Engin.* 120: 416-436.

Reed, M (1999). Sorption of anions on aluminum oxide surfaces. M.S. Thesis, Auburn University, Auburn, Alabama.

Roy, A.C. and S.K. DeDatta. (1985). Phosphate adsorption isotherms for evaluating phosphorus requirement of wetland rice soils. *Plant Soil.* 86: 185-196.

Russell, J.S., E.J. Kampath, and C.S. Andrew. (1988). Phosphorous adsorption of subtropical acid soils as influenced by the nature of the cation suite. *Soil Sci. Soc. Am. J.* 52: 1407-1410.

Sanyal, S.K. and S.K. DeDatta. (1991). Chemistry of phosphorus transformation in soils. *Adv. Soil Sci.* 16: 1-20.

Schindler, P.W., P. Liechti, and J.C. Westall. (1987). Adsorption of copper, cadmium, and lead from aqueous solution to the kaolinite/water interface. *Neth. J. Agric. Sci.* 35: 219-230.

Schindler, P.W., B. Furst, R. Dick, and P.U. wolf. (1976). Ligand properties of surface silano groups. I. Surface complex formation with Fe^{2+}, Cu^{2+}, Cd^{2+}, and Pb^{2+}. *J. Colloid Interface.* 55: 469-475.

Shaviv, A. and N. Sachar. (1989). A kinetic-mechanistic model of phosphorus sorption in calcareous soils. *Soil Sci.* 148: 172-178.

Sibbeson, E. (1981). Some new equations to describe phosphate sorption by soils. *J. Soil Sci.* 32: 67-74.

Sposito, G. (1984). The surface chemistry of soils. Oxford University Press. New York. 234.

Stumm, W.and J.J. Morgan. (1970). Aquatic chemistry : An introduction emphasizing chemical equilibria in natural waters. Wiley-Interscience . 321-326.

Stumm, W.and J.J. Morgan. (1996). Aquatic chemistry chemical equilibria in natural waters. Wiley-Interscience. 3rd edition. 293-295.

Stumm, W., C.P. Huang, and S.R. Jenkins. (1970). Specific chemical interaction affecting the stability of dispersed systems. *Croat. Chem. Acta.* 42: 223-245.

Syers, J.K., M.G. Browman, G.W. Smillie, and R.B. Corey. (1973). Phosphate sorption by soils evaluated by the langmuir adsorption equation. *Soil Sci. Am. Proc.* 37: 358-363.

Todd, G. and E. Perry. (1964). Role of silica in oxidation resistance of molybdenum disilicide. *Nature.* 202, 386.

Torrent, J. (1987). Rapid and slow phosphate sorption by Mediterranean soils: Effects of Fe oxides. *Soil Sci. Soc. Am. J.* 51: 78-82.

Van Benschoten, J.E., W.H. Young, M.R. Matsumoto, and B.E. Reed. (1998). A nonelectrostatic surface complexation model for lead sorption on soils and mineral surfaces. *J. Environ. Qual.* 27: 24-300.

Vanyukova, L.V., M. Isaeva, and B.N. Kabanova. (1962). *Dokl. Akal. Navk. SSR.* 143(2).377.

Wei, Y. and Y. Huang. (1998). Behavior of sequential extraction of lead from thermally treated lead(II)-doped alumina. *J. Environ. Qual.* 27: 343-348.

White, G.N. and L. W. Zelazny. (1986). Charge properties of soil colloids. 39-81. In D.L. Sparks (ed.) Soil physical chemistry. CRC press, Inc. Boca Raton, FL.

Wootton,P.D., M. Cheek, T.A. Kramer, and C. Lange. (1998). Treatment of heavy metal contaminated wastewater using powdered and granular alumina. *30th Mid-Atlantic Hazardous and Industrial Waste Conference Preceedings*. Villanova University, Philadelphia, Pennsylvania.

Yates, D.E., S. Levine, and T.W. Healy. (1974). Site bonding model of the electrical double layer model at the oxide/water interface. *J. Chem. Soc.*; Faraday Ttrans. I . 70: 1807-1818.

Zachara, J.M. and S.C. Smith. (1994). Edge complexation reactions of cadmium on specimen and soil-derived smectite. *Soil Sci. Soc. Am. J.* 58: 762-769.

APPENDIX A: EQUILIBRIUM PERCENTAGE REMOVED DATA

Table A.1 Lead Equilibrium Data - <74μm Mesh Alumina

No Background Matrix

pH = 2.73		pH = 4.96		pH = 7.12		pH = 8.06	
Al Conc. (g/L)	% Pb Removed	Al Conc. (g/L)	% Pb Removed	Al Conc. (g/L)	% Pb Removed	Al Conc. (g/L)	% Pb Removed
0.00	0.0	0.00	0.0	0.00	0.0	0.00	0.0
0.01	6.6	0.01	5.0	0.01	9.3	0.02	69.1
0.05	6.6	0.05	6.0	0.05	13.0	0.08	87.3
0.09	11.8	0.10	8.5	0.10	16.7	0.11	92.7
0.51	13.7	0.50	37.5	0.52	45.4	0.50	94.5
1.03	24.1	0.98	71.5	1.00	95.4	1.00	98.2
5.00	94.8	4.97	95.0	4.97	100.0	2.49	100.0
9.97	100.0	9.98	100.0	10.00	100.0	10.00	100.0

Table A.2 Lead Equilibrium Data - >1190 μm Mesh Alumina

No Background Matrix

pH = 2.57		pH = 5.17		pH = 6.81		pH = 8.06	
Al Conc. (g/L)	% Pb Removed	Al Conc. (g/L)	% Pb Removed	Al Conc. (g/L)	% Pb Removed	Al Conc. (g/L)	% Pb Removed
0.00	0.0	0.00	0.0	0.00	0.0	0.00	0.0
0.05	0.4	0.05	1.8	0.06	15.2	0.05	39.1
0.09	7.0	0.12	3.0	0.11	21.3	0.10	65.4
0.51	7.8	0.50	1.8	0.50	43.3	0.48	90.2
1.00	19.1	1.00	32.9	1.02	82.9	1.02	96.2
4.98	42.6	4.98	100.0	4.97	100.0	5.02	100.0
9.99	65.6	10.00	100.0	10.00	100.0	10.00	100.0

Table A.3 Lead Equilibrium Data - <74μm Mesh Alumina

1.0 mM Acetic Acid Background Matrix

pH = 3.55		pH = 5.83		pH = 8.93	
Al Conc. (g/L)	% Pb Removed	Al Conc. (g/L)	% Pb Removed	Al Conc. (g/L)	% Pb Removed
0.00	0.0	0.00	0.0	0.00	0.0
0.01	0.2	0.02	5.6	0.01	27.5
0.06	3.9	0.05	7.8	0.06	87.0
0.10	3.9	0.11	12.5	0.12	94.7
0.48	7.1	0.50	34.5	0.52	100.0
1.01	13.7	1.00	64.2	1.00	100.0
2.51	32.9	2.51	95.7	2.50	100.0
5.00	71.5	5.00	100.0	5.00	100.0

Table A.4 Lead Equilibrium Data - > 1190 μm Mesh Alumina

1.0 mM Acetic Acid Background Matrix

pH = 3.55		pH = 5.83		pH = 8.93	
Al Conc. (g/L)	% Pb Removed	Al Conc. (g/L)	% Pb Removed	Al Conc. (g/L)	% Pb Removed
0.00	0.0	0.00	0.0	0.00	0.0
0.05	0.2	0.06	0.5	0.05	57.3
0.11	0.2	0.11	2.7	0.09	87.8
0.50	1.5	0.50	26.7	0.51	96.2
1.01	5.4	0.99	50.2	0.98	98.5
2.53	17.8	2.51	91.4	2.48	99.2
5.03	39.9	4.98	98.6	5.00	100.0

Table A.5 Lead Equilibrium Data - <74μm Mesh Alumina

0.1 mM Sodium Chloride Background Matrix

pH = 3.20		pH = 5.57		pH = 9.15	
Al Conc. (g/L)	% Pb Removed	Al Conc. (g/L)	% Pb Removed	Al Conc. (g/L)	% Pb Removed
0.00	0.0	0.00	0.0	0.00	0.0
0.01	1.9	0.01	13.6	0.01	21.3
0.05	5.4	0.05	29.6	0.04	51.2
0.12	6.3	0.10	13.6	0.10	85.3
0.52	10.3	0.50	54.5	0.52	97.2
1.00	16.8	1.00	77.3	0.98	100.0
2.50	48.3	2.47	100.0	2.50	100.0

Table A.6 Lead Equilibrium Data - > 1190 μm Mesh Alumina

0.1 mM Sodium Chloride Background Matrix

pH = 3.20		pH = 5.57		pH = 9.15	
Al Conc. (g/L)	% Pb Removed	Al Conc. (g/L)	% Pb Removed	Al Conc. (g/L)	% Pb Removed
0.00	0.0	0.00	0.0	0.00	0.0
0.06	1.6	0.05	10.4	0.05	11.3
0.09	1.6	0.09	12.5	0.10	59.7
0.52	5.3	0.51	6.3	1.00	92.5
0.99	10.5	0.97	89.6	2.52	94.3
2.51	26.0	2.50	100.0	5.00	99.4
5.01	66.0	5.00	100.0		

APPENDIX B: KINETIC PERCENTAGE REMOVED DATA

Table B.1 Lead Kinetic Data - <74μm Mesh Alumina

No Background Matrix

	pH = 2.74	pH = 4.90	pH = 6.94
Time (min)	% Pb Removed	% Pb Removed	% Pb Removed
0.0	0.0	0.0	0.0
0.5	1.0	22.5	73.9
1.0	3.4	31.5	81.0
2.0	2.9	32.4	83.7
5.0	4.9	36.9	88.9
10.0	4.9	42.8	88.9
15.0	5.9	46.4	89.5
20.0	7.8	50.5	87.6
25.0	6.4	51.8	88.9
30.0	8.3	51.8	88.9
40.0	7.4	58.1	89.5
50.0	9.3	55.4	90.2
60.0	11.3	56.8	90.8
120.0	14.2	64.4	91.5

Table B.2 Lead Kinetic Data - >1190 μm Mesh Alumina

No Background Matrix

	pH = 2.57	pH = 5.34	pH = 6.50	pH = 10.20
Time (min)	% Pb Removed	% Pb Removed	% Pb Removed	% Pb Removed
0.0	0.0	0.0	0.0	0.0
0.5	2.5	10.4	4.8	82.0
1.0	0.5	0.6	10.9	83.0
2.0	0.5	3.9	9.1	93.0
5.0	1.0	3.9	13.9	94.0
10.0	--	--	18.2	--
15.0	0.0	13.0	21.8	89.0
20.0	1.5	14.3	26.7	95.0
25.0	1.0	--	32.1	100.0
30.0	2.0	19.5	35.8	100.0
40.0	2.0	21.4	40.6	100.0
50.0	3.0	20.1	46.1	100.0
60.0	2.5	31.8	53.9	100.0
120.0	4.0	45.5	52.7	100.0

Table B.3 Lead Kinetic Data - <74 μm Mesh Alumina

1.0 mM Acetic Acid Background Matrix

	pH = 3.46	pH = 5.80	pH = 8.43
Time (min)	% Pb Removed	% Pb Removed	% Pb Removed
0.0	0.0	0.0	0.0
0.5	1.2	12.9	6.7
1.0	4.3	15.6	--
2.0	4.3	17.8	31.1
5.0	2.9	22.8	46.7
10.0	4.8	26.2	77.8
15.0	4.8	27.2	93.3
20.0	6.0	--	86.7
25.0	7.2	36.4	88.9
30.0	8.6	30.0	--
40.0	7.0	31.9	84.4
50.0	9.1	28.0	91.1
60.0	9.8	33.2	91.1
120.0	11.0	38.4	--

Table B.4 Lead Kinetic Data - >1190 μm Mesh Alumina

1.0 mM Acetic Acid Background Matrix

	pH = 3.51	pH = 5.82	pH = 8.42
Time (min)	% Pb Removed	% Pb Removed	% Pb Removed
0.0	0.0	0.0	0.0
0.5	--	2.0	10.0
1.0	1.3	1.2	20.4
2.0	--	2.5	16.5
5.0	0.5	2.2	13.3
10.0	--	3.5	7.4
15.0	--	1.7	11.5
20.0	--	11.1	13.0
25.0	--	4.0	19.8
30.0	0.0	6.7	30.4
40.0	0.0	5.4	33.0
50.0	0.0	5.9	62.2
60.0	0.0	7.4	--
120.0	2.5	24.0	96.5

Table B.5 Lead Kinetic Data - <74 μm Mesh Alumina

0.1 mM Sodium Chloride Background Matrix

	pH = 2.77	pH = 6.78	pH = 9.58
Time (min)	% Pb Removed	% Pb Removed	% Pb Removed
0.0	0.0	0.0	0.0
0.5	3.1	41.8	84.7
1.0	0.2	47.6	84.7
2.0	2.2	49.5	80.6
5.0	1.0	51.6	90.3
10.0	4.6	52.0	94.4
15.0	3.1	53.1	98.6
20.0	3.1	49.1	97.2
25.0	3.6	54.6	100.0
30.0	3.9	53.1	100.0
40.0	4.6	53.8	100.0
50.0	5.6	52.4	100.0
60.0	5.6	50.2	100.0
120.0	12.8	--	100.0

Table B.6 Lead Kinetic Data - >1190 μm Mesh Alumina

0.1 mM Sodium Chloride Background Matrix

	pH = 2.58	pH = 6.98	pH = 9.57
Time (min)	% Pb Removed	% Pb Removed	% Pb Removed
0.0	0.0	0.0	0.0
0.5	0.7	19.3	36.5
1.0	1.2	31.2	65.3
2.0	1.4	24.8	69.4
5.0	0.0	37.1	100.0
10.0	3.4	74.3	100.0
15.0	1.2	52.0	100.0
20.0	3.1	19.8	100.0
25.0	--	31.7	100.0
30.0	2.9	73.3	100.0
40.0	2.2	74.8	100.0
50.0	4.3	76.7	100.0
60.0	2.9	64.9	100.0
120.0	6.0	96.5	100.0

APPENDIX C: EQUILIBRIUM RAW DATA

Table C.1 Lead Equilibrium Data - <74μm Mesh Alumina

No Background Matrix

pH = 2.73		pH = 4.96		pH = 7.12		pH = 8.06	
Al Conc. (g/L)	Pb Conc. (mg/L)	Al Conc. (g/L)	Pb Conc. (mg/L)	Al Conc. (g/L)	Pb Conc. (mg/L)	Al Conc. (g/L)	Pb Conc. (mg/L)
0.00	21.2	0.00	20.0	0.00	10.8	0.00	5.5
0.01	19.82	0.01	19.0	0.01	9.8	0.02	1.7
0.05	19.8	0.05	18.8	0.05	9.4	0.08	0.7
0.09	18.7	0.10	18.3	0.10	9.0	0.11	0.4
0.51	18.3	0.50	12.5	0.52	5.9	0.50	0.3
1.03	16.1	0.98	5.7	1.00	0.5	1.00	0.1
5.00	1.1	4.97	1.0	4.97	0.0	2.49	0.0
9.97	0.0	9.98	0.0	10.00	0.0	10.00	0.0

Table C.2 Lead Equilibrium Data - >1190 μm Mesh Alumina

No Background Matrix

pH = 2.57		pH = 5.17		pH = 6.81		pH = 8.06	
Al Conc. (g/L)	Pb Conc. (mg/L)	Al Conc. (g/L)	Pb Conc. (mg/L)	Al Conc. (g/L)	Pb Conc. (mg/L)	Al Conc. (g/L)	Pb Conc. (mg/L)
0.00	23.0	0.00	16.6	0.00	16.4	0.00	10.3
0.05	22.9	0.05	16.3	0.06	13.9	0.05	4.0
0.09	21.4	0.12	16.1	0.11	12.9	0.10	3.6
0.51	21.2	0.50	16.3	0.50	9.3	0.48	1.0
1.00	18.6	1.00	11.2	1.02	2.8	1.02	0.4
4.98	13.2	4.98	0.0	4.97	0.0	5.02	0.0
9.99	7.9	10.00	0.0	10.00	0.0	10.00	0.0

Table C.3 Lead Equilibrium Data - <74μm Mesh Alumina

1.0 mM Acetic Acid Background Matrix

pH = 3.55		pH = 5.83		pH = 8.93	
Al Conc. (g/L)	Pb Conc. (mg/L)	Al Conc. (g/L)	Pb Conc. (mg/L)	Al Conc. (g/L)	Pb Conc. (mg/L)
0.00	41.0	0.00	23.2	0.00	13.1
0.01	40.9	0.02	21.9	0.01	9.5
0.06	39.4	0.05	21.4	0.06	1.7
0.10	39.4	0.11	20.3	0.12	0.7
0.48	38.1	0.50	15.2	0.52	0.0
1.01	35.4	1.00	8.3	1.00	0.0
2.51	27.5	2.51	1.0	2.50	0.0
5.00	11.7	5.00	0.0	5.00	0.0

Table C.4 Lead Equilibrium Data - > 1190 μm Mesh Alumina

1.0 mM Acetic Acid Background Matrix

pH = 3.55		pH = 5.83		pH = 8.93	
Al Conc. (g/L)	Pb Conc. (mg/L)	Al Conc. (g/L)	Pb Conc. (mg/L)	Al Conc. (g/L)	Pb Conc. (mg/L)
0.00	40.9	0.00	22.1	0.00	13.1
0.05	40.8	0.06	22.0	0.05	5.6
0.11	40.8	0.11	21.5	0.09	1.6
0.50	40.3	0.50	16.2	0.51	0.5
1.01	38.7	0.99	11.0	0.98	0.2
2.53	33.6	2.51	1.9	2.48	0.1
5.03	24.6	4.98	0.3	5.00	0.0

Table C.5 Lead Equilibrium Data - <74μm Mesh Alumina

0.1 mM Sodium Chloride Background Matrix

pH = 3.20		pH = 5.57		pH = 9.15	
Al Conc. (g/L)	Pb Conc. (mg/L)	Al Conc. (g/L)	Pb Conc. (mg/L)	Al Conc. (g/L)	Pb Conc. (mg/L)
0.00	42.9	0.00	4.4	0.00	21.1
0.01	42.1	0.01	3.8	0.01	16.6
0.05	40.6	0.05	3.1	0.04	10.3
0.12	40.2	0.10	3.8	0.10	3.1
0.52	38.5	0.50	2.0	0.52	0.6
1.00	35.7	1.00	1.0	0.98	0.0
2.50	22.2	2.47	0.0	2.50	0.0

Table C.6 Lead Equilibrium Data - > 1190 μm Mesh Alumina

0.1 mM Sodium Chloride Background Matrix

pH = 3.20		pH = 5.57		pH = 9.15	
Al Conc. (g/L)	Pb Conc. (mg/L)	Al Conc. (g/L)	Pb Conc. (mg/L)	Al Conc. (g/L)	Pb Conc. (mg/L)
0.00	43.0	0.00	4.8	0.00	15.9
0.06	42.3	0.05	4.3	0.05	14.1
0.09	42.3	0.09	4.2	0.10	6.4
0.52	40.7	0.51	4.5	1.00	1.2
0.99	38.5	0.97	0.5	2.52	0.9
2.51	31.8	2.50	0.0	5.00	0.1
5.01	14.6	5.00	0.0		

APPENDIX D: KINETIC RAW DATA

Table D.1 Lead Kinetic Data - <74μm Mesh Alumina

No Background Matrix

	pH = 2.74	pH = 4.90	pH = 6.94
Time (min)	Pb Conc. (mg/L)	Pb Conc. (mg/L)	Pb Conc. (mg/L)
0.0	20.4	22.2	15.3
0.5	20.2	17.2	4.0
1.0	19.7	15.2	2.9
2.0	19.8	15.0	2.5
5.0	19.4	14.0	1.7
10.0	19.4	12.7	1.7
15.0	19.2	11.9	1.6
20.0	18.8	11.0	1.9
25.0	19.1	10.7	1.7
30.0	18.7	10.7	1.7
40.0	18.9	9.3	1.6
50.0	18.5	9.9	1.5
60.0	18.1	9.6	1.4
120.0	17.5	7.9	1.3

Table D.2 Lead Kinetic Data - >1190 μm Mesh Alumina

No Background Matrix

	pH = 2.57	pH = 5.34	pH = 6.50	pH = 10.20
Time (min)	Pb Conc. (mg/L)	Pb Conc. (mg/L)	Pb Conc. (mg/L)	Pb Conc. (mg/L)
0.0	19.8	15.4	16.5	10.0
0.5	19.3	13.8	15.7	1.8
1.0	19.7	15.3	14.7	1.7
2.0	19.7	14.8	15.0	0.7
5.0	19.6	14.8	14.2	0.6
10.0	--	--	13.5	--
15.0	19.8	13.4	12.9	1.1
20.0	19.5	13.2	12.1	0.5
25.0	19.6	--	11.2	0.0
30.0	19.4	12.4	10.6	0.0
40.0	19.4	12.1	9.8	0.0
50.0	19.2	12.3	8.9	0.0
60.0	19.3	10.5	7.6	0.0
120.0	19.0	8.4	7.8	0.0

Table D.3 Lead Kinetic Data - <74 μm Mesh Alumina

1.0 mM Acetic Acid Background Matrix

	pH = 3.46	pH = 5.80	pH = 8.43
Time (min)	Pb Conc. (mg/L)	Pb Conc. (mg/L)	Pb Conc. (mg/L)
0.0	41.7	40.4	4.5
0.5	41.2	35.2	4.2
1.0	39.9	34.1	--
2.0	39.9	33.2	3.1
5.0	40.5	31.2	2.4
10.0	39.7	29.8	1.0
15.0	39.7	29.4	0.3
20.0	39.2	--	0.6
25.0	38.7	25.7	0.5
30.0	38.1	28.3	--
40.0	38.8	27.5	0.7
50.0	37.9	29.1	0.4
60.0	37.6	27.0	0.4
120.0	37.1	24.9	--

Table D.4 Lead Kinetic Data - >1190 μm Mesh Alumina

1.0 mM Acetic Acid Background Matrix

	pH = 3.51	pH = 5.82	pH = 8.42
Time (min)	Pb Conc. (mg/L)	Pb Conc. (mg/L)	Pb Conc. (mg/L)
0.0	39.6	40.5	33.9
0.5	--	39.7	30.5
1.0	39.1	40.0	27.0
2.0	--	39.5	28.3
5.0	39.4	39.6	29.4
10.0	--	39.1	31.4
15.0	--	39.8	30.0
20.0	--	36.0	29.5
25.0	--	38.9	27.2
30.0	39.6	37.8	23.6
40.0	39.6	38.3	22.7
50.0	39.6	38.1	12.8
60.0	39.6	37.5	--
120.0	38.6	30.8	1.2

Table D.5 Lead Kinetic Data - <74 μm Mesh Alumina

0.1 mM Sodium Chloride Background Matrix

	pH = 2.77	pH = 6.78	pH = 9.58
Time (min)	Pb Conc. (mg/L)	Pb Conc. (mg/L)	Pb Conc. (mg/L)
0.0	41.4	27.3	7.2
0.5	40.1	15.9	1.1
1.0	41.3	14.3	1.1
2.0	40.5	13.8	1.4
5.0	41.0	13.2	0.7
10.0	39.5	13.1	0.4
15.0	40.1	12.8	0.1
20.0	40.1	13.9	0.2
25.0	39.9	12.4	0.0
30.0	39.8	12.8	0.0
40.0	39.5	12.6	0.0
50.0	39.1	13.0	0.0
60.0	39.1	13.6	0.0
120.0	37.3	--	0.0

Table D.6 Lead Kinetic Data - >1190 μm Mesh Alumina

0.1 mM Sodium Chloride Background Matrix

	pH = 2.58	pH = 6.98	pH = 9.57
Time (min)	Pb Conc. (mg/L)	Pb Conc. (mg/L)	Pb Conc. (mg/L)
0.0	41.4	20.2	7.4
0.5	41.1	16.3	4.7
1.0	40.9	13.9	2.7
2.0	40.8	15.2	2.2
5.0	41.4	12.7	0.0
10.0	40.0	5.2	0.0
15.0	40.9	9.7	0.0
20.0	40.1	16.2	0.0
25.0	--	13.8	0.0
30.0	40.2	5.4	0.0
40.0	40.5	5.1	0.0
50.0	39.6	4.7	0.0
60.0	40.2	7.1	0.0
120.0	38.9	0.7	0.0